# WELL TESTING INTERPRETATION
# AND
# NUMERICAL SIMULATION STUDY ON WELL KJ-20, KRAFLA

Soeroso *
UNU Geothermal Training Programme
National Energy Authority
Grensasvegur 9, 108 Reykjavik
ICELAND

* Permanent address:
PERTAMINA
Geothermal Division
Head Office, P.O. Box 12, Jakarta
INDONESIA

## ABSTRACT

The reservoir engineering techniques dealing with interpretation of well tests and simulation studies are presented for well KJ-20 at the Krafla Geothermal Field, Iceland.

These tests are both fall-off and injection tests made at the completion of the well, and build-up test after prolonged production for more than a year. The interpretation methods used consist of MDH, Horner and type curve matching. The results indicate a transmissivity in the range $1.35 \times 10^{-8}$ $m^3/P_a.s$ to $1.89 \times 10^{-8}$ $m^3/P_a.s$.

A conceptual model was made of the drainage volume for well KJ-20, Krafla. This model was then transformed for a solution with a numerical simulator to simulate and predict the future behaviour for the production from the well.

The numerical simulator, SHAFT 79 developed at the Lawrence Berkeley Laboratory at the University of California was applied for the prediction of the future reservoir behaviour in the vicinity of well KJ-20, Krafla. The simulations were processed on the VAX 11-750, VAX/VMS 4.2 computer, installed at the National Energy Authority in Reykjavik, Iceland. Two cases were considered in this study, one with the drainage volume for well KJ-20 closed on all sides and the other with the northern boundary for the drainage area open. In the closed boundary case the depletion time for well KJ-20 is about 8 years which in that case is also the depletion time for the drainage volume of the well. For the open boundary case the depletion time for well KJ-20 is increased to about 13 years. In that case the drainage volume has not been depleted.

TABLE OF CONTENTS

ABSTRACT . . . . . . . . . . . . . . . . . . . . . . . 2

1. INTRODUCTION . . . . . . . . . . . . . . . . . . . 6
   1.1. Scope of work . . . . . . . . . . . . . . . . 6
   1.2. Problem Statement . . . . . . . . . . . . . . 6

2. WELL TESTING THEORY . . . . . . . . . . . . . . . 8
   2.1. Basic Solution . . . . . . . . . . . . . . . 8
   2.2. Wellbore Storage and Skin . . . . . . . . . . 10

3. APPLICATION TO WELL KJ-20 KRAFLA . . . . . . . . . 13
   3.1. Fall-off and Injection Tests . . . . . . . . . 13
   3.2. Build-up Test . . . . . . . . . . . . . . . . 16
   3.3. Analysis and Result of Well Tests . . . . . . 20

4. SIMULATION ON WELL KJ-20 KRAFLA . . . . . . . . . 22
   4.1. Conceptual Model . . . . . . . . . . . . . . 22
   4.2. Numerical Simulation . . . . . . . . . . . . 23
   4.3. Result of Simulation . . . . . . . . . . . . 25
   4.4. Discussion . . . . . . . . . . . . . . . . . 26
   4.5. Conclusion . . . . . . . . . . . . . . . . . 27

ACKNOWLEDGEMENT . . . . . . . . . . . . . . . . . . . 28

REFERENCES . . . . . . . . . . . . . . . . . . . . . . 29

LIST OF TABLES:

Table 1 : Pressure build-up data for well KJ-20, Krafla.

Table 2 : Wellbore simulation results for well KJ-20, Krafla.

LIST OF FIGURES:

Figure 1 : Fall-off and injection test in well KJ-20, Krafla.
Figure 2 : Semilog plot of fall-off test in well KJ-20, Krafla.
Figure 3 : Type curve matching with fall-off test in well KJ-20, Krafla.
Figure 4 : Semilog plot of injection test in well KJ-20, Krafla.
Figure 5 : Type curve matching with injection test in well KJ-20, Krafla.
Figure 6 : Pressure log before well KJ-20, Krafla was shut-in.
Figure 7 : Temperature log before well KJ-20, Krafla was shut-in.
Figure 8 : Static temperature log in well KJ-20, Krafla.
Figure 9 : Horner plot for well KJ-20, Krafla.
Figure 10 : Type curve matching with build-up test in well KJ-20, Krafla.
Figure 11 : Log log plot of fall-off and injection tests in well KJ-20, Krafla.
Figure 12 : Map showing the location of well KJ-20, Krafla.
Figure 13 : Model used for simulation.
Figure 14 : The South - North section of the simulation model. A. Closed boundary ; B. Open boundary toward North.
Figure 15 : Pressure behaviour for the closed boundary case.
Figure 16 : Temperature behaviour for the closed boundary case.
Figure 17 : Vapour saturation behaviour for the closed boundary case.
Figure 18 : Enthalpy behaviour for the closed boundary case.
Figure 19 : Pressure behaviour for the open boundary case.
Figure 20 : Temperature behaviour for the open boundary case.

Figure 21 : Vapour saturation behaviour for the open boundary case.
Figure 22 : Enthalpy behaviour for the open boundary case.

**NOMENCLATURE:**

A = area, $m^2$
c = compressibility, $Pa^{-1}$
C = wellbore storage coefficient, $m^3/Pa$
g = acceleration of gravity, $m/sec^2$
h = thickness (reservoir), metre
k = permeability, $m^2$
m = slope of semilog line, Pa/cycle
P = pressure, Pa
P = changes of pressure, Pa
q = flow rate, $m^3/sec$
r = radial distance, metre
t = time, second
t = changes of time,second
V = volume, $m^3$

**Greek symbols**

ø = porosity, fraction
μ = dynamic viscosity, Pa.s
ƒ = density, $kg/m_3$

**Subscripts:**

a = apparent
A = area
D = dimensionless
f = flowing
i = initial
s = shut-in
sf = sandface
t = total
w = wellbore

# 1. INTRODUCTION

## 1.1. Scope of work

This report is the final part of the author's work during the six months training in reservoir engineering at the United Nations University (UNU) geothermal training programme at the National Energy Authority (NEA) in Reykjavik, Iceland.

The training programme as a whole included introductory lectures in various disciplines of geothermal technology such as; geology, geophysics, geochemistry, production and utilization, and reservoir engineering, for approximately six weeks. The next six weeks were spent on specialized lectures in borehole geophysics and reservoir engineering.

Before commencing the specialized training in reservoir engineering, two weeks of field excursion and seminars were undertaken which included visits to both low and high temperature geothermal fields with various types of utilization of geothermal energy. The author also obtained a brief training in the use of the IBM Personal Computer installed in the UNU.

## 1.2. Problem Statement

There are various types of tests which have been applied in geothermal wells to enhance the understanding of the reservoir behaviour. The first tests performed after well KJ-20 had reached total depth were fall-off and injection tests, both of these tests measured water level in the wellbore. The tests are conducted to obtain data that can be analyzed to get an estimate for the transmissivity and storativity in the reservoir formation.

The other test called pressure build-up test reflects the condition of a well. The results obtained from this test give an idea of the average reservoir properties, i.e quantitative value for the transmissivity in the drainage volume of the well, and mean reservoir pressure. The analysis of the test can also indicate whether the well is damaged or stimulated, and gives quantitative information concerning the shape of the reservoir either homogeneous or heterogeneous.

In order to make a prediction of the future possibilities of the reservoir behaviour in the neighborhood of well KJ-20, in the Krafla Geothermal Field, a simple conceptual model was made. The conceptual model was made on the basis of geology and data from the tests. This model was then transformed to enable a solution with a numerical simulator.

# 2. WELL TESTING THEORY

## 2.1. Basic Solution

The basic equation for transient flow in porous medium is the diffusivity equation. The diffusivity equation is a combination of the law for conservation of mass, an equation of state and Darcy's law. The diffusivity equation in radial coordinates can be written:

$$\frac{\delta^2 P}{\delta r^2} + 1/r \frac{\delta P}{\delta r} = \frac{\phi \mu c_t}{k} \frac{\delta P}{\delta t} \qquad (2.1)$$

Matthews and Russel present a derivation of the diffusivity equation and point out that it assumes horizontal flow, negligible gravity effect, a homogeneous and isotropic porous medium and a single fluid of small and constant compressibility. The parameters $\mu$, $\phi$, $c_t$ and k are assumed independent of pressure.

In dimensionless form, pressure drop can be written:

$$P_D (t_D, r_D) = \frac{2 \pi k h}{q \mu} (P_i - P(t,r)) \qquad (2.2)$$

In transient flow, $P_D$ is always a function of dimensionless time, which is when based on wellbore radius:

$$t_D = \frac{k t}{\phi \mu c_t r_w^2} \qquad (2.3)$$

or when based on drainage area

$$t_{DA} = \frac{k t}{\phi \mu c_t A} = t_D \left(\frac{r_w^2}{A}\right) \qquad (2.4)$$

Dimensionless pressure also varies with location in the reservoir, as indicated in equation (2.2) by dimensionless radial distance from the operating well. The radial dimensionless distant is defined as:

$$r_D = \frac{r}{r_w} \qquad (2.5)$$

Substitution of these variables into the radial diffusivity equation gives:

$$\frac{\delta^2 P_D}{\delta r_D^2} + \frac{1}{r_D}\frac{\delta P_D}{\delta r_D} = \frac{\delta P_D}{\delta t_D} \qquad (2.6)$$

The dimensionless diffusivity equation can then be solved for the appropriate initial and boundary condition (Earlougher 1977, S.P. Kjaran 1982, Sigurdsson. O, lectures).

During the initial transient flow period, it has been found that the well can for most practical purposes be approximated by a line source. This assumes that in comparison to the apparently infinite reservoir, the wellbore radius is negligible and the wellbore itself can be treated as line source. For the infinite acting reservoir the boundary and initial condition are given as:

$$P_D = 0 \qquad \text{at} \quad t_D = 0 \;, \quad \text{for all} \quad r_D$$

$$P_D = 0 \qquad \text{at} \quad r_D = \quad , \quad \text{for all} \quad t_D$$

$$\lim_{r_D \quad 0} r_D \left(\frac{\delta P_D}{\delta r_D}\right) = 1 \qquad t_D \gg 0$$

The solution to the radial diffusivity equation with these boundary and initial conditions is the exponential integral solution to the flow equation (also called the line source or Theis solution). The exponential integral solution is:

$$P_D\ (t_D, r_D) = -\tfrac{1}{2}\ E_i\left(\frac{-\ r_D^2}{4\ t_D}\right) \qquad (2.7)$$

or

$$P_D\ (t_D, r_D) = \tfrac{1}{2}\left[\ \ln\left(\frac{t_D}{r_D^2}\right) + 0.80907\ \right] \qquad (2.8)$$

$$\text{for} \quad \frac{t_D}{r_D^2} \geq 100$$

The difference between equation 2.7 and equation 2.8 is only about two percent, when $t_D/r_D^2 \geq 5$.
At the operating well (in a single well system) $r_D = 1$, so $t_D/r_D^2 = t_D$ and equation 2.8 becomes:

$$P_D(t_D) - s = \tfrac{1}{2} [\ln t_D + 0.80907] \qquad (2.9)$$

Substitution for the dimensionless parameters into equation 2.9.

$$(P_i - P(t,r)) = \frac{q\mu}{4\pi k h} [\ln(\frac{k t}{\phi c_t r_w^2}) + 0.80907 + 2s] \qquad (2.10)$$

or

$$P_{wf} = P_i \pm 0.183 \frac{q\mu}{k h} [\log t + \log(\frac{k}{\phi \mu c_t r_w^2}) + 0.3514 + 0.8686s] \qquad (2.11)$$

where: + for injection
- for production

## 2.2. Wellbore Storage and Skin

**Wellbore Storage:**

Wellbore storage also called after flow, after production, after injection, and wellbore loading or unloading, has long been recognized as effecting short time transient pressure behaviour (Earlougher,1977). This effect exists in the well when the well is opened for production, the fluid flow from the well is larger than the corresponding flow from the reservoir into the well.

Similarly when the well is shut-in, fluid still continues to pass through the sandface into the hole. Wellbore storage is characterized by a wellbore constant, defined as:

$$C = \frac{\Delta V}{\Delta P} \qquad (2.12)$$

For the wellbore with changing liquid level, the wellbore constant is:

$$C = \frac{V_u}{\rho g} \qquad (2.13)$$

where: $V_u$ is the wellbore volume per unit length.

The dimensionless wellbore storage coefficient, $C_D$ is defined as:

$$C_D = \frac{C}{2 \pi \phi c_t h r_w^2} \qquad (2.14)$$

The sandface flow rate at the formation can be calculated from the following equation:

$$q_{sf} = q + C \frac{dP_w}{dt} \qquad (2.15)$$

and

$$q_{sf} = q \left[ 1 - C_D \frac{d}{dt_D} P_D (t_D, C_D, \ldots) \right] \qquad (2.16)$$

In logarithmic term:

$$\log \frac{q_{sf}}{q} = - \log C_D - \log \Delta P_D + \log \Delta t_D$$

or

$$\log \Delta t_D = \log \Delta P_D + \log C_D + \log \left( \frac{q_{sf}}{q} \right) \qquad (2.17)$$

At the beginning of a well test the sandface flow is approximately zero , so the wellbore storage constant can be found from a straight line with slope in the early time data on a log log plot of pressure change, $\Delta P$ versus elapsed time, $\Delta t$. The wellbore storage coefficient, can then be calculated from:

$$C = q \frac{\Delta t}{\Delta P} \qquad (2.18)$$

The diffusivity equation including wellbore storage in the well was solved by Everdingen and Hurst (1949) for the infinite reservoir case.In that case the inner boundary condition for equation 2.6 are changed to:

$$\lim_{r_D \quad 0} r_D \frac{\delta P_D}{\delta r_D} = 1 - C_D \frac{\delta P_D}{\delta t_D} \qquad (2.19)$$

Skin Effect.

The skin characterizes the condition of the well, in terms of damaged or stimulated. These conditions can be described with additional pressure drop in the reservoir near the well. According to van Everdingen (1953) the additional pressure drop close to the well is defined:

$$P = \frac{\Delta q \mu}{2 \pi k h} s \qquad (2.20)$$

From the skin factor an apparent wellbore radius can also be determined as:

$$r_{wa} = r_w e^{-s} \qquad (2.21)$$

A positive skin factor therefore indicates that the well is damaged or has solid deposition near the well face. A negative value for the skin factor, on the other hand indicates that permeability is higher near the well commonly due to sections of oversized hole, removal of debris from permeable zones or intersection of fractures.

## 3. APPLICATION TO WELL KJ-20 KRAFLA

### 3.1. Fall-off and Injection Tests

Well KJ-20 was drilled during June - August 1982 with directional drilling (N 12.6 E) and cut fracture at 1270 meter depth. A 13 3/8 " casing were set to 212.5 meter depth, 9 5/9 " casing to 650 meter depth and completed with 7 " blind and slotted liner from 596.20 meter (liner hanger) to 1762.7 meter. The total depth of well KJ-20 was 1823 meter. This well was finished with a completion test. The test were both fall-off test and injection test.

**Well completion procedure:** Before starting the completion test, pressure gauge was lowered into the well to certain depth with water still pumped into the well at a rate of 25.76 l/s. The first fall-off test started on the 20$^{th}$ of August 1982 at 17:08 with initial pressure 15.24 bar at 200 meters depth and finished after approximately 8 hours (484 minutes). Then followed by an injection test which started on August 21, 1982 at 01:26 with an injection rate of 30.86 l/s. This test was carried out for approximately 7 hours (431 minutes). A second fall-off test was performed after the injection was stopped which lasted for about 93 minutes. These tests are illustrated as shown in Figure 1.

**The aim of completion test:** The aim of the completion test (fall off and injection ) is to reveal the condition or characteristics of the well. These conditions or characteristics of the well can be shown from calculation result i.e transmissivity, formation storativity, wellbore storage and skin factor. The result can indicate whether the well has a good or poor potential and also if the well is damaged or stimulated.

**Analysis:** The completion test of well KJ-20 Krafla was analyzed using Miler, Dykes and Hutchinson (MDH) method. This method involves graphing the pressure during the test versus logarithm of the time. For comparision type curve match were also used for this test.

**Fall-off test:**

**MDH method:** Changes of pressure or declining pressure after pumping was stopped are plotted versus logarithm of time as shown in Figure 2. A straight line can be fitted to the data which gives a slope m equal to 2.5 bar/cycle. From equation 2.11 the transmissivity of well KJ-20 can be calculated as follows:

**equation 2.11:**

$$P_{wf} = P_i - 0.1832 \frac{q\,\mu}{k\,h} \left[\log t + \log \left(\frac{k}{\phi\,\mu\,c_t\,r_w^2}\right) + 0.3514 + 0.8686\,s\right]$$

with the slope : $m = 0.1832 \frac{q\,\mu}{k\,h}$

The injection rate prior to the fall-off test was 25.76 l/s or 0.0257 $m^3/s$.

The transmissivity: $\frac{k\,h}{\mu} = 0.1832 \frac{q}{m}$

$$\frac{k\,h}{\mu} = \frac{0.1832 \times 0.02576}{2.5 \times 10^5}$$

$$\frac{k\,h}{\mu} = 1.89 \times 10^{-8} \ m^3/Pa.s$$

**Type curve match:** The changes of pressure (delta P) versus changes of time (delta t) are plotted on log log paper (Figure 3). From type curve match for infinite acting reservoir with skin and wellbore storage the following match points were obtained:

| | | |
|---|---|---|
| $C_D$ = 1 E+05 | P = 6.0 bar | t = 47.5 minutes |
| s = - 5 | $P_D$ = 3 | $t_D = 4.0 \times 10^6$ |

Then from equation 2.2 we have:

$$P_D = \frac{2 \pi k h}{q \mu} P$$

$$\frac{k h}{\mu} = \frac{q}{2 \pi} \left( \frac{P_D}{P} \right)_{M.P}$$

transmissivity: $\frac{k h}{\mu} = \frac{0.02576 \times 3}{2 \pi \; 6.0 \times 10_5} = 2.05 \times 10^{-8} \; m^3/Pa.s$

And from equation 2.3:

$$t_D = \frac{k t}{\phi \mu c_t r_w^2}$$

storativity: $\phi c_t h = \frac{k h}{\mu r_w^2} \left( \frac{t}{t_D} \right)_{M.P}$

$$\phi c_t h = \frac{2.05 \times 10^{-8} \times 47.5 \times 60}{0.012 \times 4.0 \times 10^6} = 1.12 \times 10^{9} \; m/Pa$$

**Injection test:**

**MDH method:** The MDH plot is shown in Figure 4, and the straight line gives a slope m = 3.6 bar/cycle. Following the same procedure as for the fall-off test :

$$m = 0.1832 \frac{q \mu}{k h}$$

and the injection rate during the test was 30.86 l/s or 0.03086 $m^3/s$.

Then the transmissivity is: $\frac{k\,h}{\mu} = 0.1832 \frac{q}{m}$

$$\frac{k\,h}{\mu} = \frac{0.1832 \times 0.03086}{3.6 \times 10^5} = 1.57 \times 10^{-8}\ m^3/Pa.s$$

**Type curve match:** The changes of pressure (delta P) versus the changes of time (delta t) during the injection test are plotted on log log paper as shown in Figure 5. From type curve match for infinite acting reservoir with skin and wellbore storage one obtains:

$C_D$ = 1E+05    P = 6.6 bar    t = 47 minutes

s = - 5    $P_D$ = 3    $t_D = 4.0 \times 10^6$

with the same procedure as for the fall-off test using equation 2.2 and equation 2.3 one obtains:

transmissivity: $\frac{k\,h}{\mu} = \frac{q}{2\,\pi} \left(\frac{P_D}{P}\right)_{M.P}$

$$\frac{k\,h}{\mu} = \frac{0.03086 \times 3}{2\,\pi \times 6.6 \times 10^5} = 2.23 \times 10^{-8}\ m^3/Pa.s$$

and

storativity: $\phi\, c_t\, h = \frac{k\,h}{\mu\, r_w^2} \left(\frac{t}{t_D}\right)_{M.P}$

$$\phi\, c_t\, h = \frac{2.23 \times 10^{-8} \times 47 \times 60}{4.0 \times 10^6} = 1.3 \times 10^{-9}\ m/Pa$$

## 3.2. Build-up Test

The production from well KJ-20, Krafla was initiated on October 5, 1982 and continued for more than a year. A break in electrical power generation from the Krafla Geothermal Power Plant was planned beginning from May to early September

1984 (Sigurdsson et al.,1985). Therefore well KJ-20 was shut-in on June 6,1984 and pressure build-up monitored.

**Procedure:** Before closing the well for build-up test, pressure and temperature logs were made to determine the setting depth for the pressure gauge to ensure the setting depth to be below water level and the main feed point, see Figure 6 and Figure 7. This was done on June 1, 1984 and the well was shut in for about one hour during each log and then put in production again until June 6, 1982.

**The aim of the test:** The aim of the build-up test was as for the completion test to reveal the condition or characteristics of the well after it had been producing for more than a year and also to compare the results, with parameters determined from the completion test. In this case Horner plot and type curve matching method were used for determine reservoir parameters.

**Data:** The pressure build-up data is tabulated in Table 1. Because of lack of flowing pressure at the feed zone at the time of shut-in, a wellbore simulator (Ambastha wellbore simulation program) was used to simulate the flowing condition of the well before shut-in with total flow rate as 10.6 kg/s and discharge fluid enthalpy as 1929 kJ/kg at 11.7 bar well head pressure. The wellbore simulation results are shown in table 2.

For well KJ-20 the discharge enthalpy exceeds the enthalpy of water at the maximum reservoir temperature of 302.6°C (see Figure 8) i.e: $h_w$ = 1382 kJ/kg. It is therefore assumed that two phase fluid mixture enters the well and for evaluating the reservoir parameters the mixture density is used.

**Horner plot:**
When the well was shut-in, the response of the bottom-hole shut-in pressure can be expressed by using the prinsiple of superposition in time. For a well producing at rate q until time t, and at zero rate thereafter. The effect of this on pressure

build-up can be looked on as if an imaginary well located at the same point started injecting with the same rate as the prior production rate. Earlougher 1977 described that the pressure at any time after shut-in as:

$$P_{ws} - P_i = 2\ m\ \{\ P_D\ (t + \quad t)_D - P_D\ (\quad t_D)\ \}$$

From equation 2.9:

$$P_D\ (t_D) - s = \tfrac{1}{2}\ [\ \ln t_D + 0.80907\ ]$$

Assuming that the logarithmic approximation to the dimensionless pressure solution applies, and the equation for the shut-in pressure can be written as:

$$P_{ws} - P_i = m\ [\ \log\ (t + \quad t) - \log \quad t\ ]$$

or

$$P_{wf} - P_i = m\ [\ \log \frac{t + \quad t}{t}\ ]$$

Where :

$$m = -\ 0.1832\ \frac{q\ \mu}{k\ h}$$

The static pressure during the build-up is plotted versus the logarithm of the time ratio (the sum of production time and shut-in time divided by shut-in time) as shown in Figure 9. From this graph the average reservoir pressure can be found by extrapolating the straight line to log (t +  t)/  t equal one. For well KJ-20 this pressure is 98 bar, for the slope m = 11.7 bar/cycle.

It is assumed that the fluid flow in the well is isoenthalpic (the enthalpy of the fluid entering the well is equal to the flowing enthalpy at the surface). For that case one obtains (from the steam tables) at 99 bara: $H_s$ = 2726.5 kJ/kg; $H_w$ = 1403.2 kJ/kg; $\rho_s$ = 54.79 kg/m$^3$; $\rho_w$ = 690.15 kg/m$^3$.
The mixture density is given by Grant et al.,1982

$$\frac{1}{\rho_t} = \frac{x}{\rho_s} + \frac{1-x}{\rho_w}$$

And

$$x = \frac{H_t - H_w}{H_s - H_w}$$

Where: $x$ = steam fraction; $H_t$ = total discharge enthalpy, kJ/kg; $H_s$ = steam enthalpy, kJ/kg; $H_w$ = water enthalpy, kJ/kg.

For our case

$$x = \frac{1929 - 1403.2}{2726.5 - 1403.2} = 0.3973$$

$$\frac{1}{\rho_t} = \frac{0.3973}{54.79} + \frac{(1 - 0.3973)}{690.15}$$

$$\rho_t = 123.08 \quad kg/m^3$$

Flow rate before the well was shut-in was 10.6 kg/s which corresponds to (10.6)/(123.08) = 0.086 $m^3/s$, and with the slope m = 11.7 bar/cycle.

$$\frac{k\,h}{\mu} = 0.1832\,\frac{q}{m} = \frac{0.1832 \times 0.086}{11.7 \times 10^5}$$

$$\frac{k\,h}{\mu} = 1.35 \times 10^{-8} \quad m^3/P_a.s$$

**Type curve match:**

From the type curve match shown in Figure 10, for infinite reservoir with skin and wellbore storage the following is obtained at the match point:

$C_D$ = 1E+05 ; $t_D = 2.0 \times 10^7$ ; $t = 3.0 \times 10^2$ hrs

s = -5 ; $P_D$ = 3.8 ; P = 64 bars

Based on equations 2.2 and 2.3 and following the same procedure as for the completion test one obtains:

Transmissivity: $\frac{k\,h}{\mu} = \frac{q}{2\pi} \left(\frac{P_D}{P}\right) = \frac{0.1832 \times 3.8}{2\pi\, 64 \times 10^5}$

$$\frac{k\,h}{\mu} = 0.832 \times 10^{-8} \quad m^3/P_a.s$$

Storativity : $\phi\, c_t\, h = \frac{k\,h}{\mu\, r_w^2} \left(\frac{t}{t_D}\right)$ ; $r_w = 0.1095$ m

$$\phi\, c_t\, h = \frac{0.832 \times 10^{-8} \times 3.0 \times 10^2 \times 3600}{0.012 \times 2.0 \times 10^7}$$

$$\phi\, c_t\, h = 3.744 \times 10^{-8} \quad m/P_a$$

## 3.3. Analysis and Result of Well Tests

The completion test both the injection and fall-off test indicate that well KJ-20, Krafla is connected to a high conductivity fracture.

This indication can be observed in the early time data on the log log plot of delta P versus delta t (log log straight line of half slope), see Figure 11.

The injection test in Figure 11 shows oscilation at a certain point, which in this case may be caused of reservoir behaviour (i.e temperature effect). Homogeneous behaviour can also been seen in the log log shape during the completion test, which corresponds to an infinite acting behavior.

From the completion test it is very difficult to determine or to predict the nature of the outer boundary from the late time data, because of the short duration of the test.

The magnitute of transmissivity from the fall-off test is $2.36 \times 10^{-8}$ $m^3/P_a.s$ and from the injection test $1.57 \times 10^{-8}$

$m^3/P_a.s$ using MDH method and the magnitute of transmissivity from the pressure build up test is $1.35 \times 10^{-8}$ $m^3/P_a.s$ using Horner plot which is not very different from the former two.

The formation storativity of the pressure build-up test is approximately ten times greater than from the completion test, which in this case indicates the presence of more compressible two phase fluid in the reservoir at the time of the build-up test.

# 4. SIMULATION ON WELL KJ-20 KRAFLA

## 4.1. Conceptual Model

In order to simulate the reservoir behaviour in the vicinity of well KJ-20 Krafla a simple conceptual model was made. The model is based on geological, production output and reservoir parameters from the Krafla area (Sudurhlidar). An aerial overview of the Krafla Geothermal field and the location of well KJ-20 can be seen in Figure 12. Based on the conceptual model and the output potential of well KJ-20 and its surrounding wells, the simplified three dimensonal reservoir model, and the South - North section used in the simulation were made as shown in Figure 13 and 14 respectively. Different boundary conditions were used in order to give some ideas about the possible reservoir behaviour that may occur in the future. Two cases were selected as follow:

**Closed boundary:**

To simulate the reservoir behaviour in the vicinity of well KJ-20, Krafla, a drainage area of fixed shape was selected. The shape of the drainage area was selected in accordance with the ratio of the today output potential for the neighbouring production wells at the Sudurhlidar Field. These neighbouring wells confine the boundaries of the drainage area to the East, South and West. To the North an existing East-West fracture marks the northern boundaries for the drainage area. This model has an area of 0.124 $km^2$. The drainage volume is made up of 200 meter thick caprock, and a 2000 meter thick reservoir rock. For this case all the boundaries were taken as closed boundaries.
The reservoir domain is divided into four layers each 500 meter thick. Circular elements with 50 meter radius are imbedded in the center layers of the reservoir domain. Furthermore the lower circular element encloses another circular element with 10 meter radius and the sink is emplaced in it. The model for the simulation study in this case consists therefore of three materials for the three domains including atmosphere. They are

divided into 9 elements varying in size from 1.0 x $10^7$ $m^3$ to 1.0 x $10^{20}$ $m^3$ with 13 interface connections between them.

The initial conditions for this case are described in section 4.2.

**Open boundary:**

This model is the same as for the closed boundary case, but the north boundary is now open and connects to a fracture which is further open to a large reservoir element to the north. This model therefore, consists of 4 materials for the various reservoir domains. They are divided into 16 elements varying in size and volume from 1 x $10^7$ $m^3$ to 1 x $10^{30}$ $m^3$ with 32 interface connections between elements. The initial temperature and pressure conditions of the large reservoir element used in this study were put as 320 °C and 114 bar, respectively.

## 4.2. Numerical Simulation

To run the simulation some assumptions were made as:

1. All of the material for the various reservoir domains is assumed to have the same value for rock density and porosity.

2. The caprock thickness is assumed 200 m and reservoir thickness is assumed 2000 m divided into 4 layers with the same thickness (500 m).

3. Relative permeability in fractured media were assumed to be linear functions of vapour saturation.

4. No recharge is from the basement to the system.

5. Constant conditions are kept at the surface.

**Data for the numerical simulation.**

1. Total production of well KJ-20 is 10.6 kg/s, based on measurement of the well output before shut-in with well head pressure 11.7 bar gauge and total discharge fluid enthalpy 1929 kJ/kg.

2. The values used for rock density and porosity are 2650 kg/m$^3$ and 5% (Bodvarsson et al., 1982) and are assumed the same for all of the zones.

3. The initial conditions for pressure and temperature were taken from average pressure and temperature profiles in the Krafla field (Sudurhlidar). The values used correspond to the depth to the center of each layer and it assumed that initially there is no boiling in the reservoir. Then the initial pressure and temperature conditions for the sink at 1350 meter depth are 114 bar and 320 °C (Bodvarsson et al., 1982).

4. Permeability was taken from the result of the injection test analysis (Bodvarsson et al., 1982),i.e: 2.0 x $10^{-15}$ m$^2$, and it assumed that horizontal and vertical permeability are the same. This value is only valid for the reservoir domains. For the caprock permeability was estimated 2.0 x $10^{-18}$ m$^2$, this value was used for both horizontal and vertical directions.

   Permeability of the fracture was guessed as 2.0 x $10^{-14}$ m$^2$ in the horizontal direction and 1.0 x $10^{-14}$ m$^2$ in the vertical direction. The guessed values for the fracture permeability were suggested by Omar Sigurdsson.

5. The values of irreducible liquid saturation, irreducible vapour saturation and perfectly mobile vapour saturation were taken from Bodvarsson et al., 1982 i.e: 35% , 5% and 65% respectively.

6. Thermal conductivity of caprock is 1.5 J/m.s.°C and 1.7 J/m.s.°C for fracture and reservoir rocks (Bodvarsson et al.,1982).

7. Heat capacity of all materials for the various reservoir domains were taken as: 1000 J/kg °C (Bodvarsson et al., 1982). In these simulation studies, the computer program SHAFT 79 from the Lawrence Berkeley Laboratory, University of California (K. Pruess and R:C Schoeder, 1980) was used to simulate the reservoir behaviour of the drainage volume for well KJ-20, Krafla i.e: pressure, temperature, vapour saturation and discharge enthalpy. The simulation processing was done on the VAX 11-750, VAX/VMS 4.2 computer, installed at the National Energy Authority in Reykjavik, Iceland.

## 4.3. Result of Simulation

The changes in some of the reservoir parameters during the simulation studies of well KJ-20 Krafla for both the closed boundary and the open boundary cases are summarized in Figure 15 to Figure 22.

**Closed Boundary**

Pressure and temperature in the outer elements seem to decrease slowly and vapour saturation increases gradually with time but in the sink element pressure and temperature quickly drop within the first few months of production and continue to decrease drastically with time. From the initiation of production in the sink element, vapour saturation falls rapidly and fluctuates up to a period of 1 year. This is due to encroachment of fluids from outer element into sink element at the initiation of production.

Vapour saturation and enthalpy behaviour in the sink element remains constant from the fourth year until the eighth year. This is because boiling is depressed in the sink element due to increasing flow of cooler fluid from the layer above, and decreasing of lateral fluid flow from the surrounding.

The vapour saturation for both outer element and sink element representing well KJ-20 Krafla reaches a maximum value (100%) in 8.3 years, see Figure 17. At that time the pressure in the sink element has dropped to 3.62 bar as shown in Figure 15, and well KJ-20 is depleted.

Open Boundary

The simulation results for the open boundary case are characterized by slowly decreasing pressure and temperature in the outer element which continuous until the end of simulation. Maximum pressure drop in the outer element from the beginning to the end of simulation is 28 bar and maximum temperature drop is 21°C. In the sink element both pressure and temperature rapidly drop from the beginning to the end of simulation.

From Figure 21 vapour saturation in the outer element reaches a maximum value of 80.17% but vapour saturation in the sink element reaches a maximum value of 100% in 13 years. When the vapour saturation in the sink element has reached 100% the pressure quickly drops as well KJ-20 is depleted, as shown in Figure 19.

## 4.4. Discussion

In the simple model used in this simulation studies, the sink element was embedded within a larger circular element, which in the open boundary case had a small common interface with the fracture, Actually from drilling reports for well KJ-20, Krafla, the well intersects fracture at 1270 m depth. If the sink element would have been placed interface with the fracture or in the fracture itself the result would most likely indicate a longer depletion time for well KJ-20 than the present study gives.

From the initiation of production in the sink element for both the closed and the open boundary case the pressure and temperature drop rapidly. This is because the model used in the simulation study is very coarse, especially for the open boundary case where the large reservoir to the north is simulated by one element. These pressure and temperature behavior would be smoother if the large reservoir element in the north would be divided into layers like for the main drainage volume.

## 4.5. Conclusion

The results of the simulation study indicate that well KJ-20 in the Krafla Geothermal Field has a depletion time of 8 years for the closed boundary case and 13 years for the open boundary case under the condition of no recharge from the basement to the production element, 5% porosity (Bodvarsson et al., 1982), and a 500 meter thick production zone.

The simulation study gives also information or ideas about the reponses for well KJ-20 in the Krafla Geothermal Field (Sudurhlidar) that may occur in the future.

ACKNOWLEDGEMENT

I would like to convey my deep gratitude to Mr. Omar Sigurdsson for his diligent supervision and guidance in the specialized training, the National Energy Authority of Iceland for releasing the data from the Krafla Geothermal Field (well KJ-20), Mr. Jon Steinar Guðmundsson the Director of United Nations University Geothermal Training Programme for his excellent organization of the 1986 training session.

Special thanks are due to the PERTAMINA management for granting me six months leave of absence to pursue this valuable training.

REFERENCES

1. Abaneth Wale (1985): Reservoir Engineering Study of The Krafla - Hvitholar Geothermal Area, Iceland., Report 1985.

2. Asgrimur Gudmundsson, Benedikt Steingrimsson, Gudjon Gudmundsson, Gudmundur O. Freidleifsson, Hilmar Sigvaldsson, Omar Sigurdsson, Steinar P. Gudlaugsson and Valgardur Stefansson (1983): Krafla Well KJ-20 Report; vol 1 - 4, in Iceland., Desember 1982 - February 1983.

3.Charles B. Haukwa (1985): Analysis of Well Test Data in The Olkaria West Geothermal Field Kenya., Report 1985.

4. Gudmundur S. Bodvarsson and Sally M. Benson, Omar Sigurdsson and Volgardur Stefansson, Einar T. Eliasson (1984): The Krafla Geothermal Field, Iceland vol 1 - 4., Water Resources Research., Novenber 1984.

5. H. J. Ramey. Jr: Reservoir Engineering Assessment of Geothermal System, Department of Petroleum Engineering Stanford University.,1981.

6. Jaime Ortiz - Ramizes (1983); Two Phase Flow in Geothermal Wells: Development and Uses of a Computer Code., June 1983.

7. Kjaran S.P and Elliason J. (1983): Geothermal Reservoir Engineering Lecture notes UNU, Iceland.

8. K. Pruess and R.C Schroeder (1980): SHAFT 79 User's Manual, Lowrence Berkely Laboratory University of California Berkely, California 94720., March 1980.

9. Malcom A. Grant, Tony Donaldson, Paul F. Bixley (1982): Geothermal Reservoir Engineering.,1982.

10. Omar Sigurdsson, Benedikt S. Steingrimsson and Steffansson (1985): Pressure Build Up Monitoring of The Krafla Geothermal

Field, Iceland, Tenth Workshop on Geothermal Reservoir Engineering Standford University, January 22 - 24., 1985.

11. Pratomo Harry (1979): Build Up Test Analysis of Ngawha and Kamojang Wells, report., November 1979.

12. R.A. Dawe and D.C. Wilson (1985): Development in Petroleum Engineering - 1., 1985.

13. Robert C. Earlouger. Jr (1977): Advances in Well Test Analysis.,1977.

14. Sulaiman Syafei (1982): Kawah Kamojang Reservoir Simulation, report., November 1982.

Table 1: Pressure build up data for well KJ-20

| Date | Time | Pressure bar | Depth m | Temperature °C | Flowrate l/s |
|---|---|---|---|---|---|
| 840606 | 1112 | ----- | ------ | 268.70 | 13.80 |
| 840606 | 1230 | 43.50 | 1300.00 | 268.70 | 0.00 |
| 840606 | 1655 | 56.54 | 1300.00 | 268.70 | 0.00 |
| 840607 | 1850 | 66.50 | 1300.00 | 268.70 | 0.00 |
| 840608 | 1120 | 69.44 | 1300.00 | 268.70 | 0.00 |
| 840613 | 1105 | 76.43 | 1300.00 | 294.40 | 0.00 |
| 840621 | 0132 | 79.84 | 1300.00 | 294.90 | 0.00 |
| 840715 | 1123 | 84.54 | 1300.00 | 299.90 | 0.00 |
| 840809 | 1734 | 86.83 | 1300.00 | 299.90 | 0.00 |

data run for Krafla-20

INFUT DATA AS FOLLOW:

| | |
|---|---|
| WATER GRAVITY | 1.0000 |
| TOTAL MASS FLOWRATE,LB/HR | 84142.8000 |
| HEAT TRANSF COEFF,BTU/HR/SQ | 0.0000 |

AT THE WELLHEAD :

| | |
|---|---|
| DEPTH,FT | 0.00 |
| PRESSURE,PSIA | 184.20 |
| TEMPERATURE,F | 374.91 |

PIPE DIAMETER USED AS FOLLOW:

FROM 0.0 FT TO 1956.1 FT, PIPE DIAMETER (FT) = 0.7500
APS ROUGHNESS (FT) = 0.0005

FROM 1956.1 FT TO 4265.0 FT, PIPE DIAMETER (FT) = 0.5830
ABS ROUGHNESS (FT) = 0.0006

TOTAL LENGTH DIVIDED IN 50 INTERVALS

DOWNHOLE SHUT-IN TEMPERATURE AS FOLLOW:

| DEPTH,FT | TEMP,F |
|---|---|
| 1312.40 | 414.70 |
| 1968.00 | 480.60 |
| 2625.00 | 514.60 |
| 3281.00 | 541.00 |
| 3609.00 | 553.00 |
| 3937.00 | 563.00 |

** PRESSURE ANALYSIS **

| | |
|---|---|
| TOTAL FRICTION, LIQUID | = 0.0000 PSI |
| TOTAL POTENTIAL, LIQUID | = 0.0000 PSI |
| TOTAL FRICTION, TWO-PHASE | = 82.3398 PSI |
| TOTAL POTENTIAL, TWO-PHASE | = 28.1337 PSI |
| TOTAL ACCELE., TWO-PHASE | = 0.6716 PSI |

* TWO-PHASE FLOW *

| DEPTH,FT | PRES,PSIA | TEMP,F | EH,BTU/LB | FRICTION Psi/100ft | ACCELE. Psi/100ft | POTENTIAL Psi/100ft | STM.FRAC | REGIME | aw/A ft/s | as/A ft/s |
|---|---|---|---|---|---|---|---|---|---|---|
| 0.00 | 184.20 | 374.91 | 829.20 | | | | 0.5654 | | | |
| 85.30 | 185.40 | 375.42 | 829.20 | 0.7882 | 0.0056 | 0.4218 | 0.5651 | TRAN | 0.4187 | 73.8562 |
| 170.60 | 186.59 | 375.96 | 829.20 | 0.7866 | 0.0055 | 0.4217 | 0.5647 | TRAN | 0.4192 | 73.3700 |
| 255.90 | 187.79 | 376.49 | 829.20 | 0.7849 | 0.0054 | 0.4218 | 0.5644 | TRAN | 0.4197 | 72.8624 |
| 341.20 | 188.98 | 377.02 | 829.20 | 0.7832 | 0.0053 | 0.4220 | 0.5640 | TRAN | 0.4202 | 72.3620 |
| 426.50 | 190.17 | 377.55 | 829.20 | 0.7814 | 0.0053 | 0.4222 | 0.5637 | TRAN | 0.4207 | 71.8688 |
| 511.80 | 191.36 | 378.04 | 829.20 | 0.7797 | 0.0052 | 0.4226 | 0.5633 | TRAN | 0.4211 | 71.4102 |
| 597.10 | 192.54 | 378.56 | 829.20 | 0.7778 | 0.0051 | 0.4230 | 0.5630 | TRAN | 0.4216 | 70.9306 |
| 682.40 | 193.73 | 379.08 | 829.20 | 0.7760 | 0.0050 | 0.4235 | 0.5626 | TRAN | 0.4221 | 70.4577 |
| 767.70 | 194.91 | 379.60 | 829.20 | 0.7741 | 0.0050 | 0.4242 | 0.5623 | TRAN | 0.4226 | 69.9914 |
| 853.00 | 196.10 | 380.08 | 829.20 | 0.7722 | 0.0049 | 0.4248 | 0.5620 | TRAN | 0.4230 | 69.5584 |
| 938.30 | 197.28 | 380.59 | 829.20 | 0.7703 | 0.0048 | 0.4256 | 0.5616 | TRAN | 0.4235 | 69.1047 |
| 1023.60 | 198.46 | 381.09 | 829.20 | 0.7683 | 0.0048 | 0.4265 | 0.5613 | TRAN | 0.4239 | 68.6569 |
| 1108.90 | 199.64 | 381.59 | 829.20 | 0.7662 | 0.0047 | 0.4274 | 0.5610 | TRAN | 0.4244 | 68.2158 |
| 1194.20 | 200.82 | 382.06 | 829.20 | 0.7642 | 0.0046 | 0.4284 | 0.5607 | TRAN | 0.4249 | 67.7802 |
| 1279.50 | 201.99 | 382.56 | 829.20 | 0.7621 | 0.0046 | 0.4294 | 0.5603 | TRAN | 0.4253 | 67.3764 |
| 1364.80 | 203.17 | 383.06 | 829.20 | 0.7601 | 0.0045 | 0.4306 | 0.5600 | TRAN | 0.4258 | 66.9525 |
| 1450.10 | 204.34 | 383.55 | 829.20 | 0.7578 | 0.0045 | 0.4318 | 0.5597 | TRAN | 0.4262 | 66.5342 |
| 1535.40 | 205.52 | 384.04 | 829.20 | 0.7558 | 0.0044 | 0.4331 | 0.5593 | TRAN | 0.4267 | 66.1215 |
| 1620.70 | 206.69 | 384.49 | 829.20 | 0.7538 | 0.0044 | 0.4345 | 0.5590 | TRAN | 0.4271 | 65.7392 |
| 1706.00 | 207.86 | 384.98 | 829.20 | 0.7515 | 0.0043 | 0.4359 | 0.5587 | TRAN | 0.4276 | 65.3371 |
| 1791.30 | 209.03 | 385.46 | 829.20 | 0.7494 | 0.0043 | 0.4374 | 0.5584 | TRAN | 0.4280 | 64.9403 |
| 1876.60 | 210.21 | 385.94 | 829.20 | 0.7471 | 0.0042 | 0.4389 | 0.5580 | TRAN | 0.4285 | 64.5487 |
| 1961.90 | 211.38 | 386.39 | 829.20 | 0.7150 | 0.0041 | 0.4405 | 0.5577 | TRAN | 0.4289 | 64.1622 |
| 2047.20 | 213.86 | 387.39 | 829.20 | 2.0000 | 0.0236 | 0.4970 | 0.5571 | MIST | 0.7110 | 105.2428 |
| 2132.50 | 216.33 | 388.35 | 829.20 | 1.9795 | 0.0229 | 0.5032 | 0.5564 | MIST | 0.7125 | 103.9412 |
| 2217.80 | 218.78 | 389.33 | 829.20 | 1.9602 | 0.0223 | 0.5091 | 0.5558 | MIST | 0.7140 | 102.7189 |
| 2303.10 | 221.22 | 390.29 | 829.20 | 1.9408 | 0.0216 | 0.5152 | 0.5551 | MIST | 0.7155 | 101.4973 |
| 2388.40 | 223.65 | 391.21 | 829.20 | 1.9226 | 0.0211 | 0.5210 | 0.5545 | MIST | 0.7170 | 100.3504 |
| 2473.70 | 226.06 | 392.15 | 829.20 | 1.9044 | 0.0205 | 0.5270 | 0.5538 | MIST | 0.7185 | 99.2023 |
| 2559.00 | 228.47 | 393.04 | 829.20 | 1.8868 | 0.0199 | 0.5329 | 0.5532 | MIST | 0.7199 | 98.0985 |
| 2644.30 | 230.86 | 393.95 | 829.20 | 1.8689 | 0.0194 | 0.5390 | 0.5526 | MIST | 0.7213 | 96.9735 |
| 2729.60 | 233.24 | 394.82 | 829.20 | 1.8515 | 0.0187 | 0.5451 | 0.5521 | MIST | 0.7228 | 95.8777 |
| 2814.90 | 235.60 | 395.71 | 829.20 | 1.8350 | 0.0184 | 0.5510 | 0.5515 | MIST | 0.7241 | 94.8154 |
| 2900.20 | 237.98 | 396.60 | 829.20 | 1.8347 | 0.0181 | 0.5586 | 0.5509 | TRAN | 0.7255 | 93.8002 |
| 2985.50 | 240.48 | 397.49 | 829.20 | 1.9454 | 0.0187 | 0.5771 | 0.5503 | TRAN | 0.7269 | 92.7829 |
| 3070.80 | 243.12 | 398.46 | 829.20 | 2.0624 | 0.0192 | 0.5981 | 0.5496 | TRAN | 0.7284 | 91.6983 |
| 3156.10 | 245.89 | 399.43 | 829.20 | 2.1778 | 0.0197 | 0.6204 | 0.5490 | TRAN | 0.7299 | 90.6165 |
| 3241.40 | 248.80 | 400.48 | 829.20 | 2.2983 | 0.0203 | 0.6455 | 0.5483 | TRAN | 0.7315 | 89.4716 |
| 3326.70 | 251.86 | 401.54 | 829.20 | 2.4163 | 0.0207 | 0.6718 | 0.5475 | TRAN | 0.7332 | 88.3324 |
| 3412.00 | 255.06 | 402.67 | 829.20 | 2.5378 | 0.0212 | 0.7012 | 0.5468 | TRAN | 0.7350 | 87.1356 |
| 3497.30 | 258.41 | 403.82 | 829.20 | 2.6556 | 0.0216 | 0.7320 | 0.5460 | TRAN | 0.7368 | 85.9493 |
| 3582.60 | 261.90 | 405.00 | 829.20 | 2.7753 | 0.0219 | 0.7659 | 0.5452 | TRAN | 0.7387 | 84.7120 |
| 3667.90 | 265.55 | 406.25 | 829.20 | 2.8900 | 0.0222 | 0.8011 | 0.5444 | TRAN | 0.7406 | 83.4899 |
| 3753.20 | 269.35 | 407.50 | 829.20 | 3.0048 | 0.0224 | 0.8395 | 0.5435 | TRAN | 0.7426 | 82.2255 |
| 3838.50 | 273.29 | 408.82 | 829.20 | 3.1135 | 0.0226 | 0.8792 | 0.5426 | TRAN | 0.7447 | 80.9824 |
| 3923.80 | 277.37 | 410.15 | 829.20 | 3.2181 | 0.0228 | 0.9209 | 0.5418 | TRAN | 0.7468 | 79.7350 |
| 4009.10 | 281.60 | 411.50 | 829.20 | 3.3226 | 0.0228 | 0.9667 | 0.5408 | TRAN | 0.7490 | 78.4291 |
| 4094.40 | 285.98 | 412.92 | 829.20 | 3.4213 | 0.0229 | 1.0146 | 0.5399 | TRAN | 0.7513 | 77.1273 |
| 4179.70 | 290.49 | 414.33 | 829.20 | 3.5145 | 0.0229 | 1.0647 | 0.5389 | TRAN | 0.7536 | 75.8271 |
| 4265.00 | 295.15 | 415.77 | 829.20 | 3.6035 | 0.0228 | 1.1182 | 0.5379 | TRAN | 0.7560 | 74.4986 |

Table 2 : Wellbore simulation results for well KJ-20, Krafla

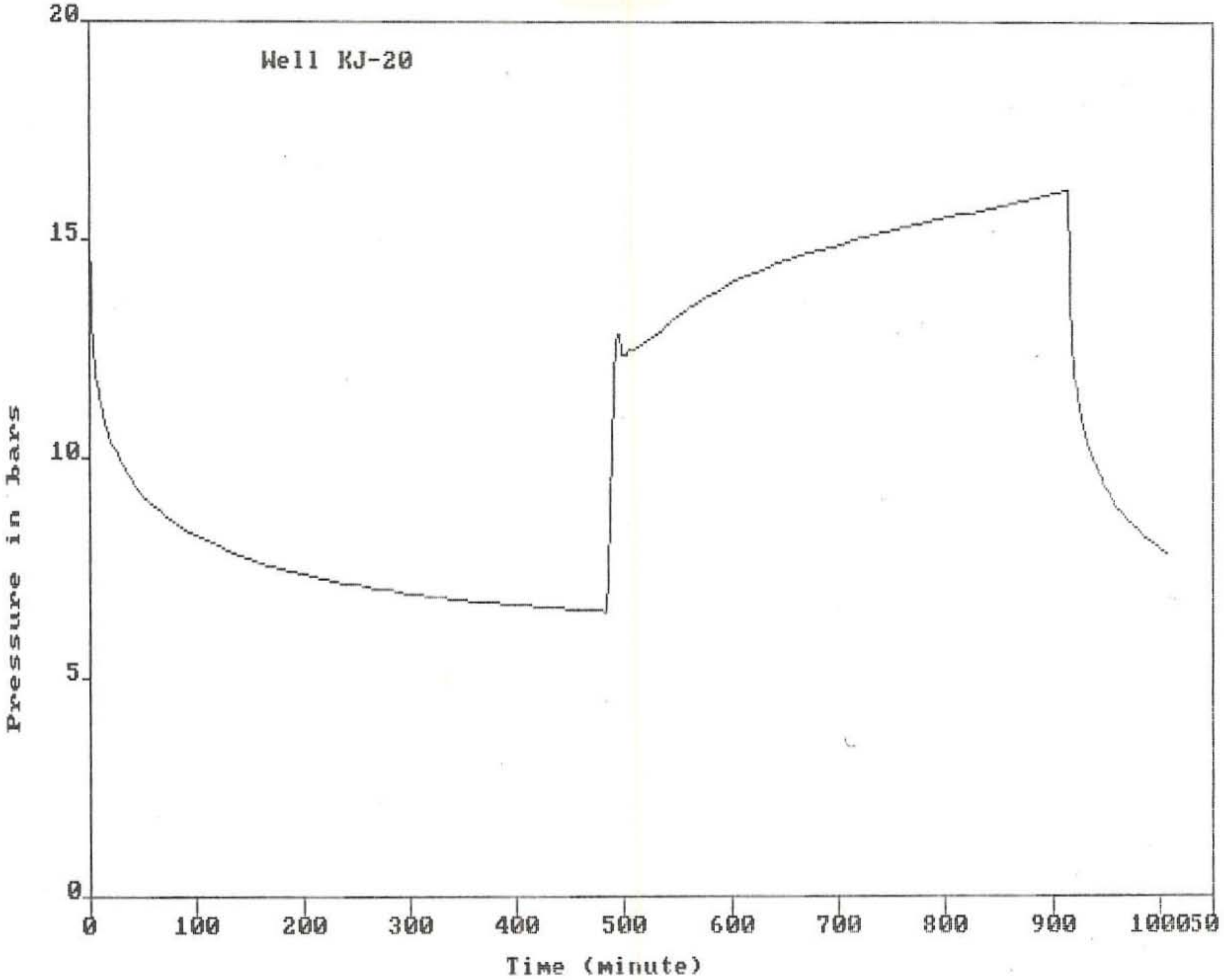


Figure 1 : Fall-off and injection test in well KJ-20, Krafla.

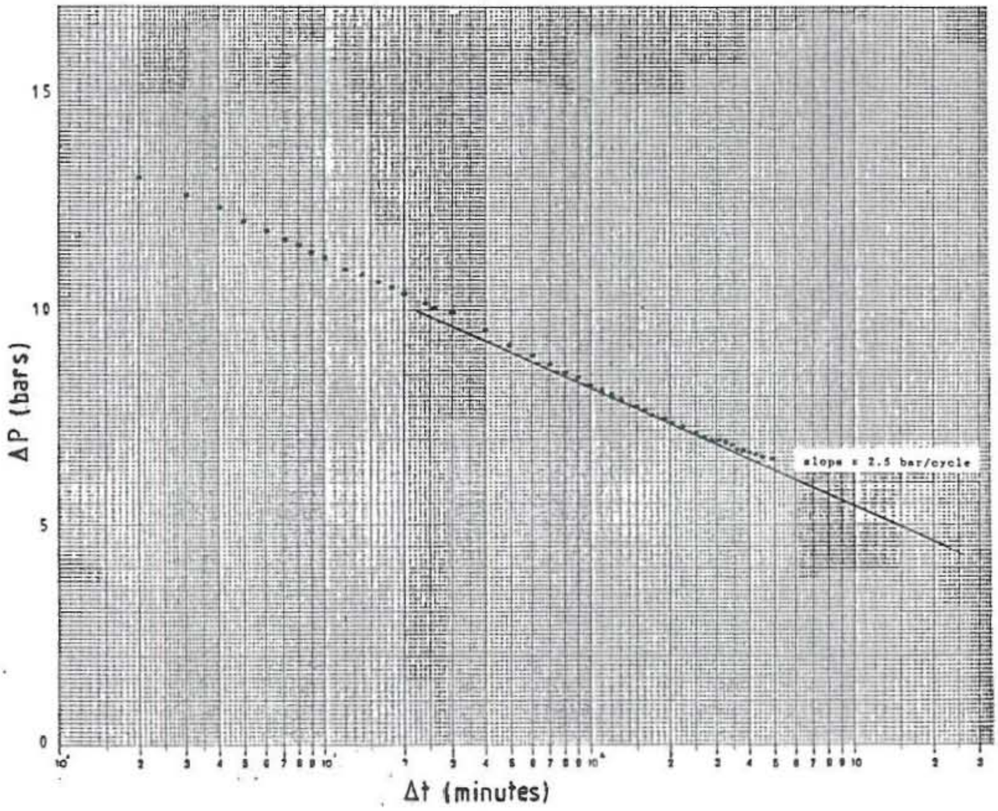


Figure 2 : Semilog plot of fall-off test in well KJ-20, Krafla.

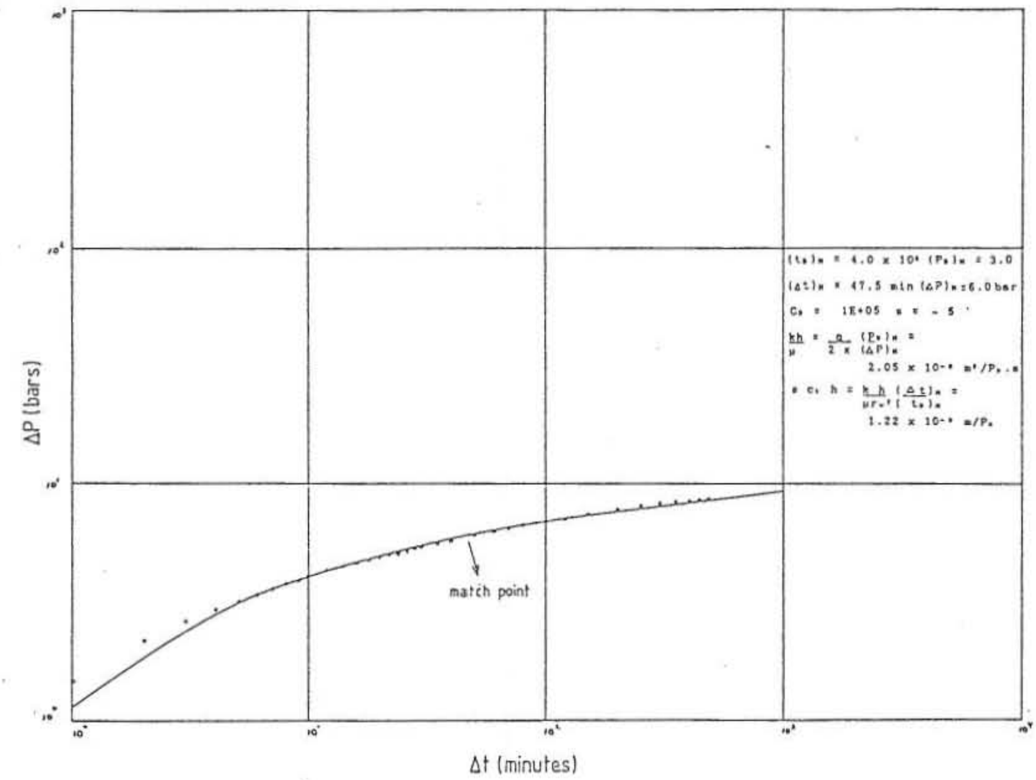


Figure 3 : Type curve matching with fall-off test in well KJ-20, Krafla.

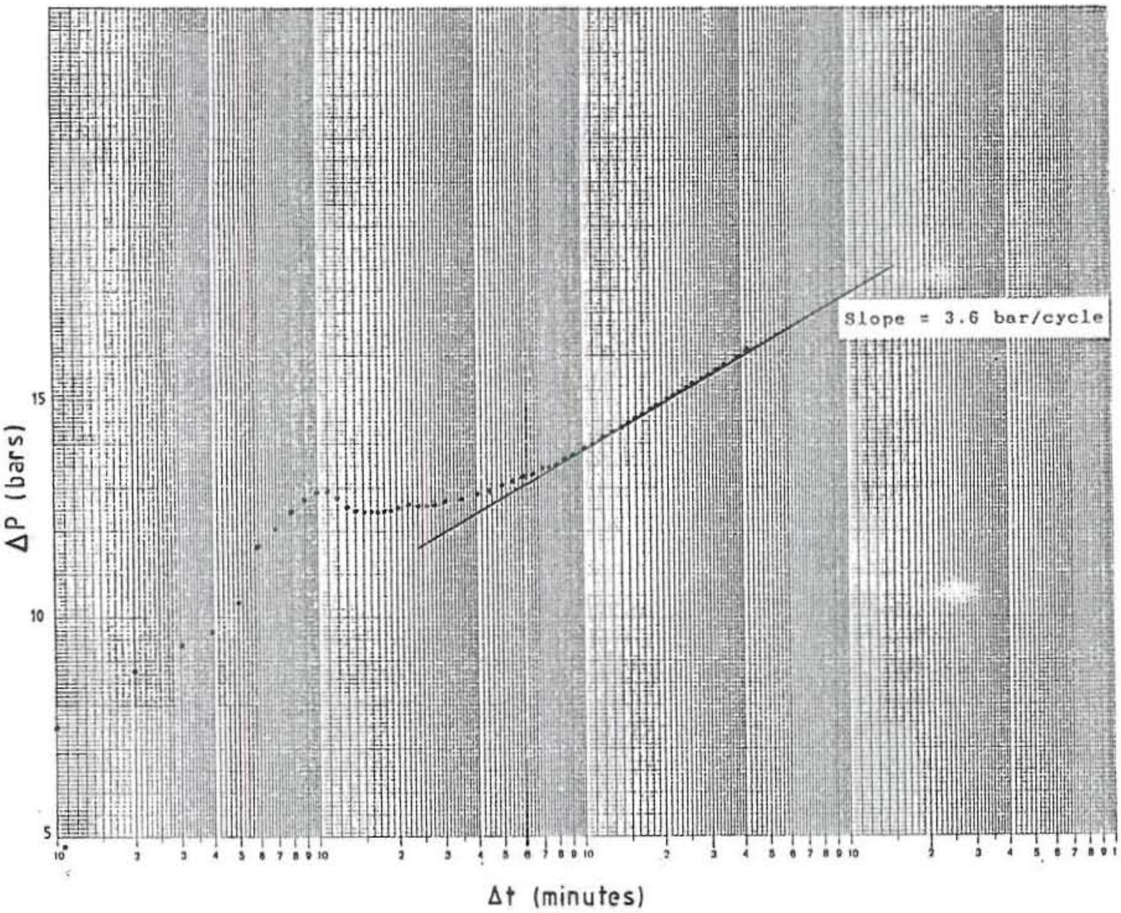


Figure 4 : Semilog plot of injection test in well KJ-20, Krafla.

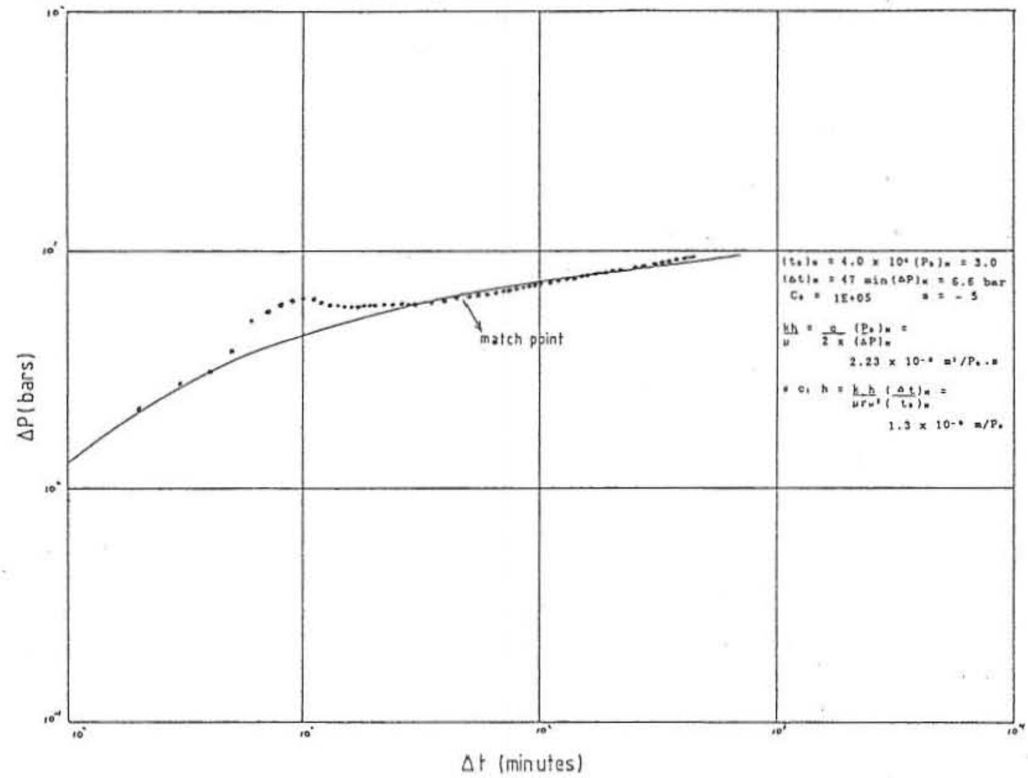


Figure 5 : Type curve matching with injection test in well KJ-20, Krafla.

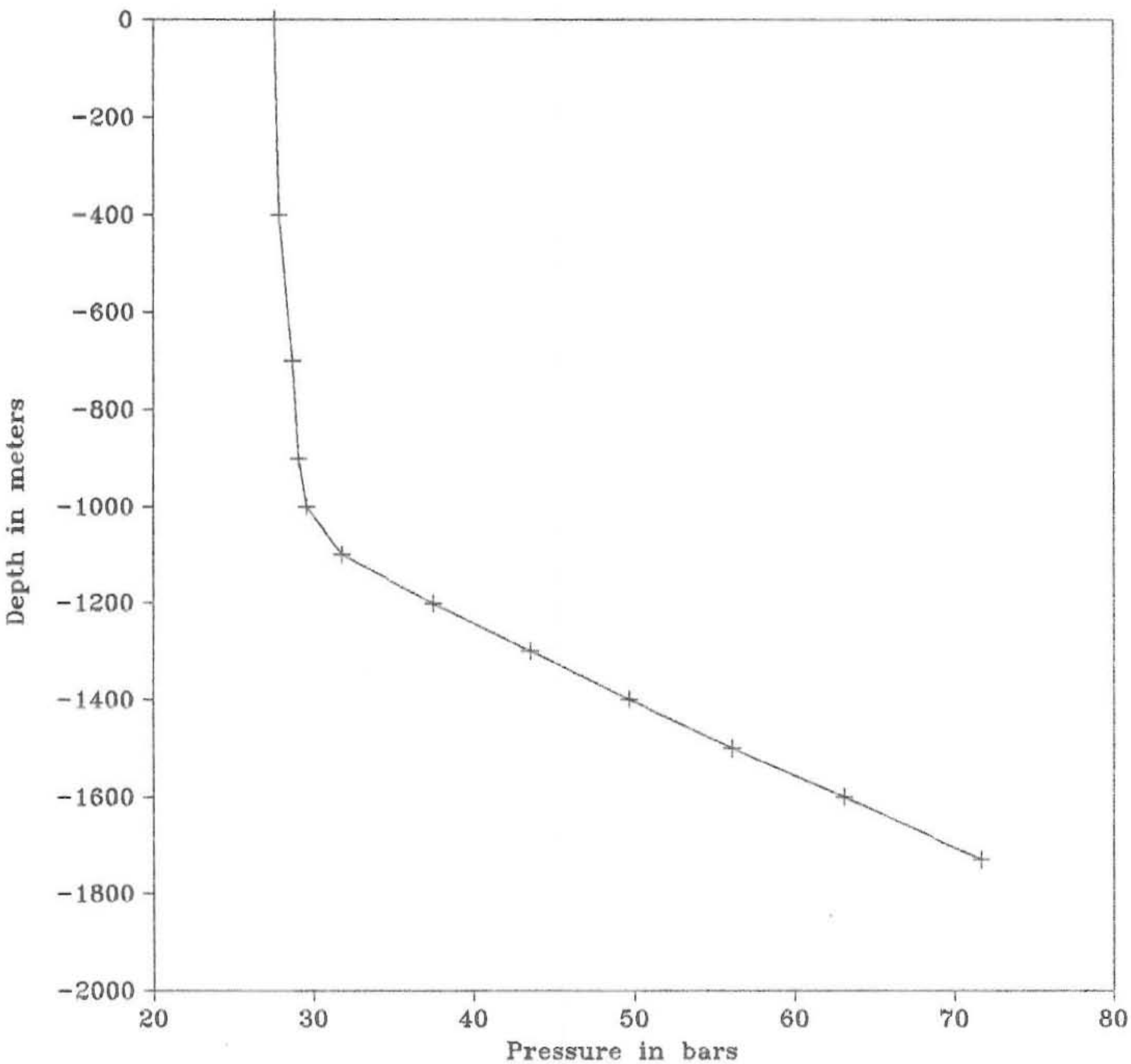


Figure 6 : Pressure log before well KJ-20, Krafla was shut-in.

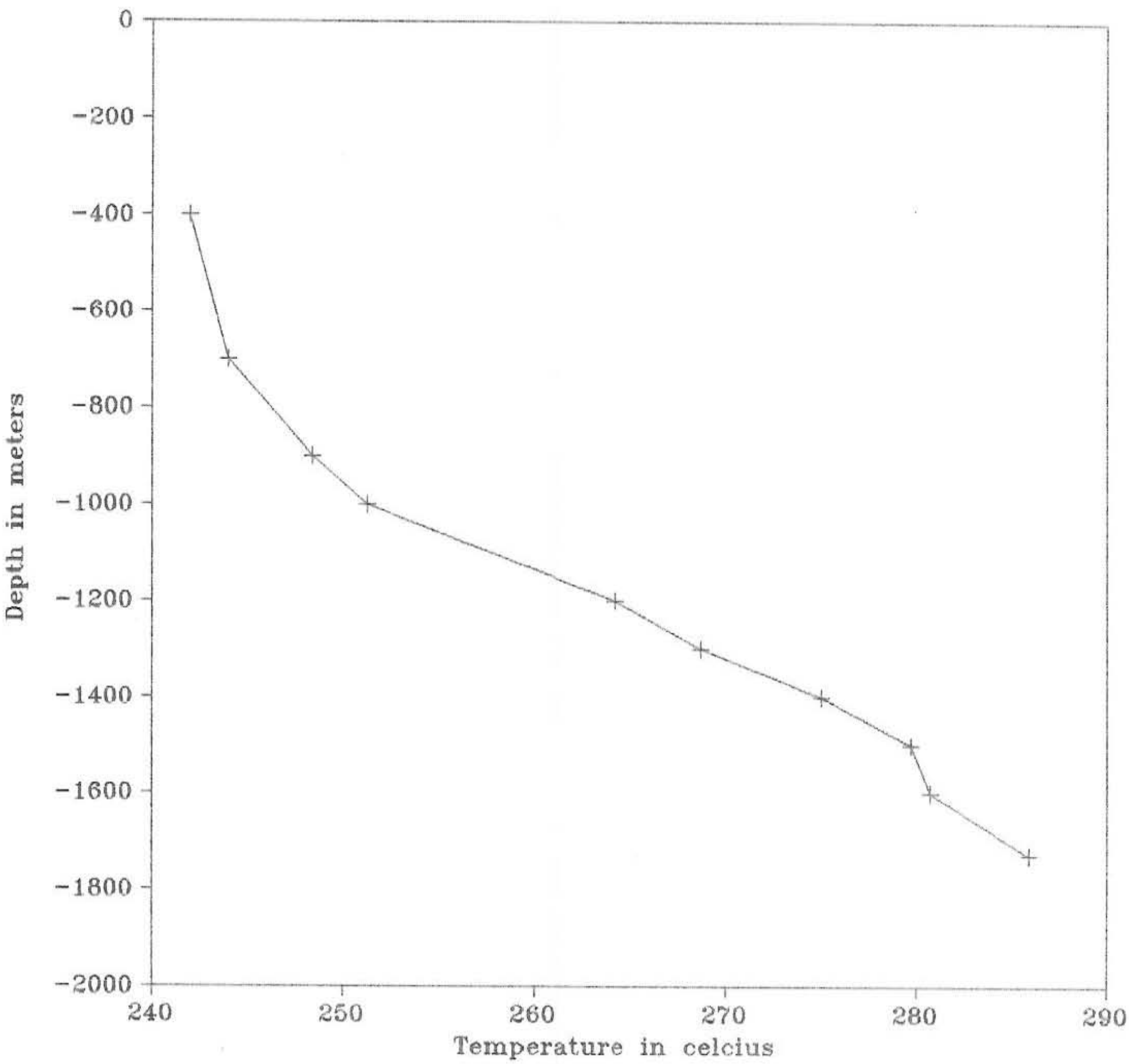


Figure 7 : Temperature log before well KJ-20, Krafla was shut-in.

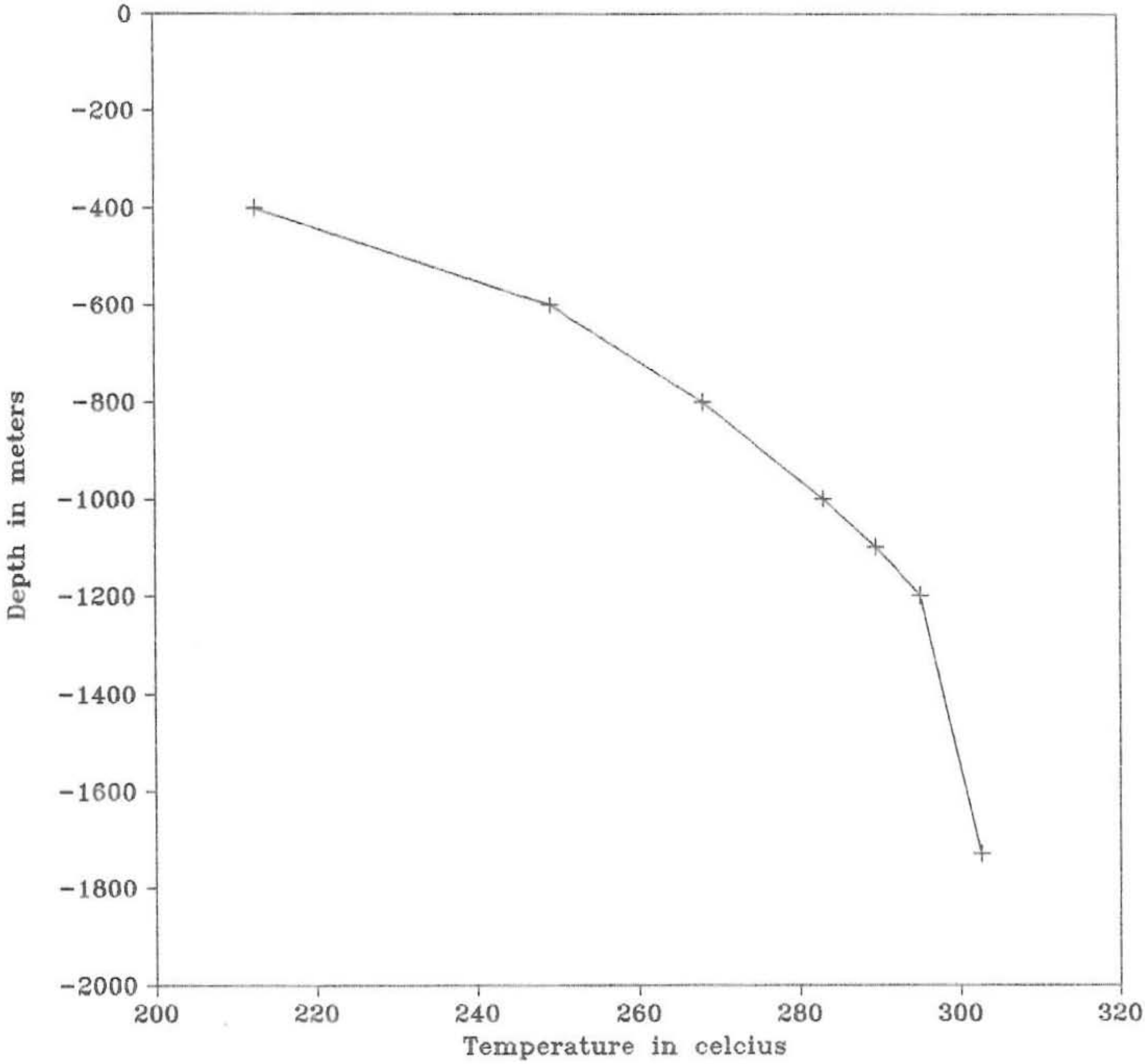


Figure 8 : Static temperature log in well KJ-20, Krafla.

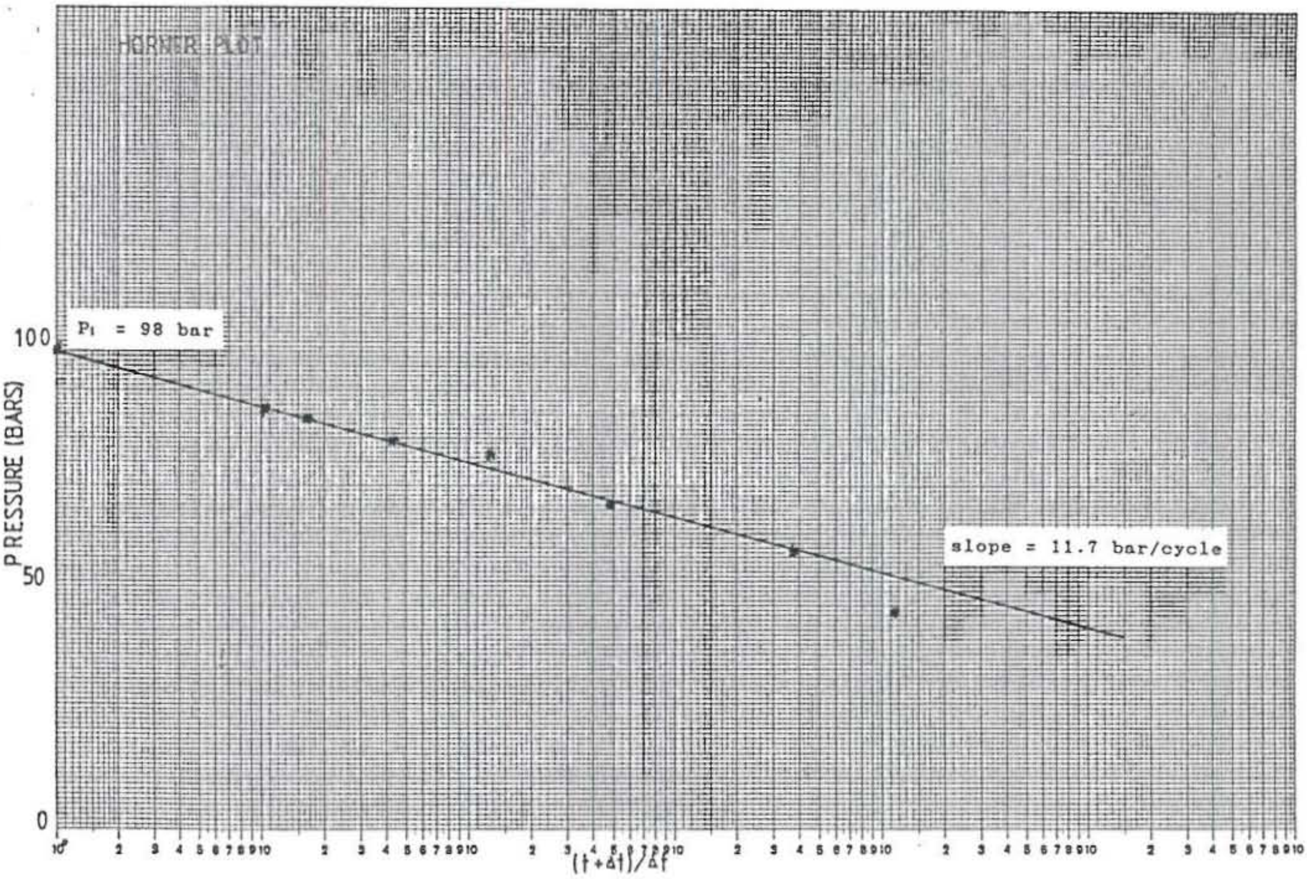


Figure 9: Horner plot for well KJ-20, Krafla.

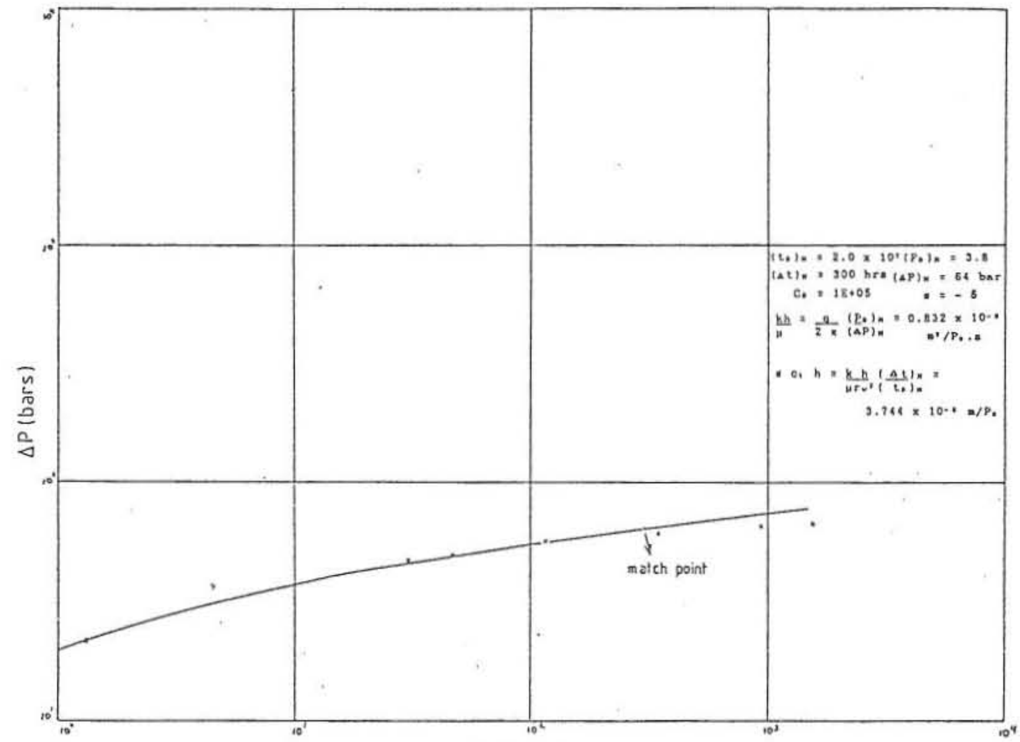


Figure 10 : Type curve matching with build-up test in well KJ-20, Krafla.

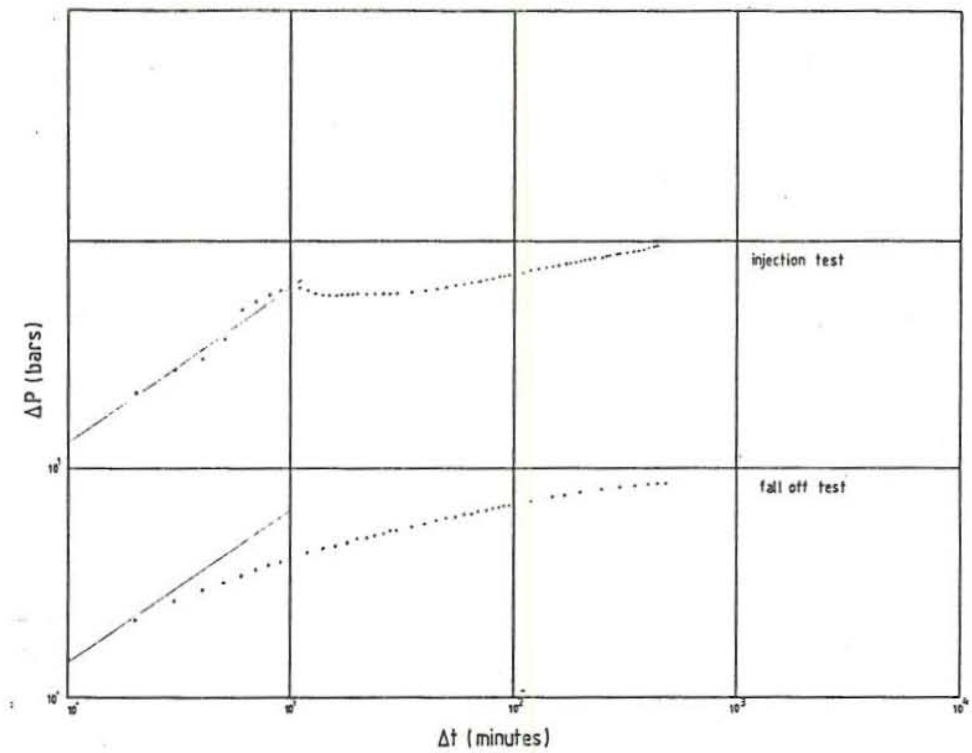


Figure 11 : Log log plot of fall-off and injection tests in well KJ-20, Krafla.

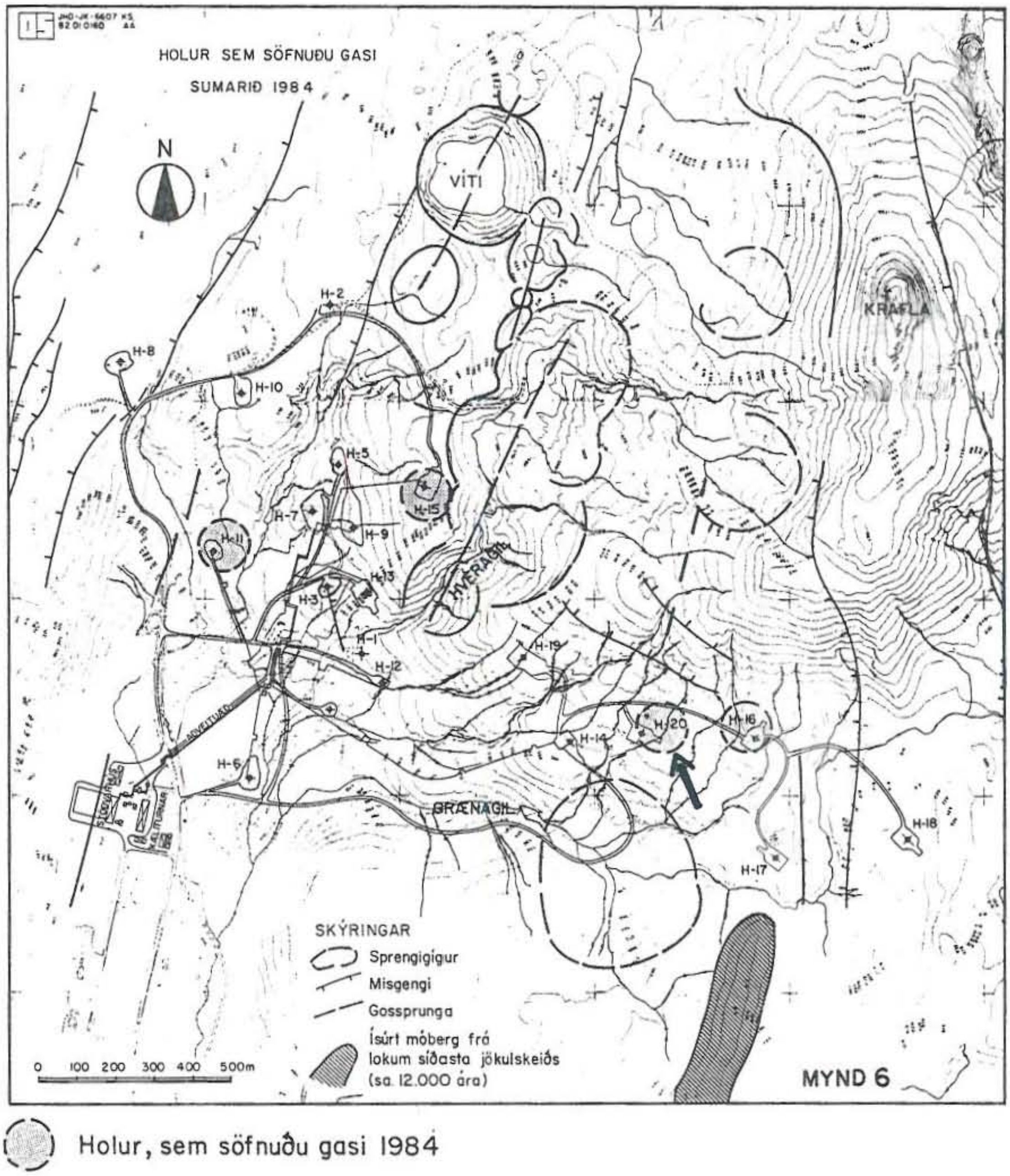


Figure 12: An aerial overview of the Krafla field and the location of well KJ-20.

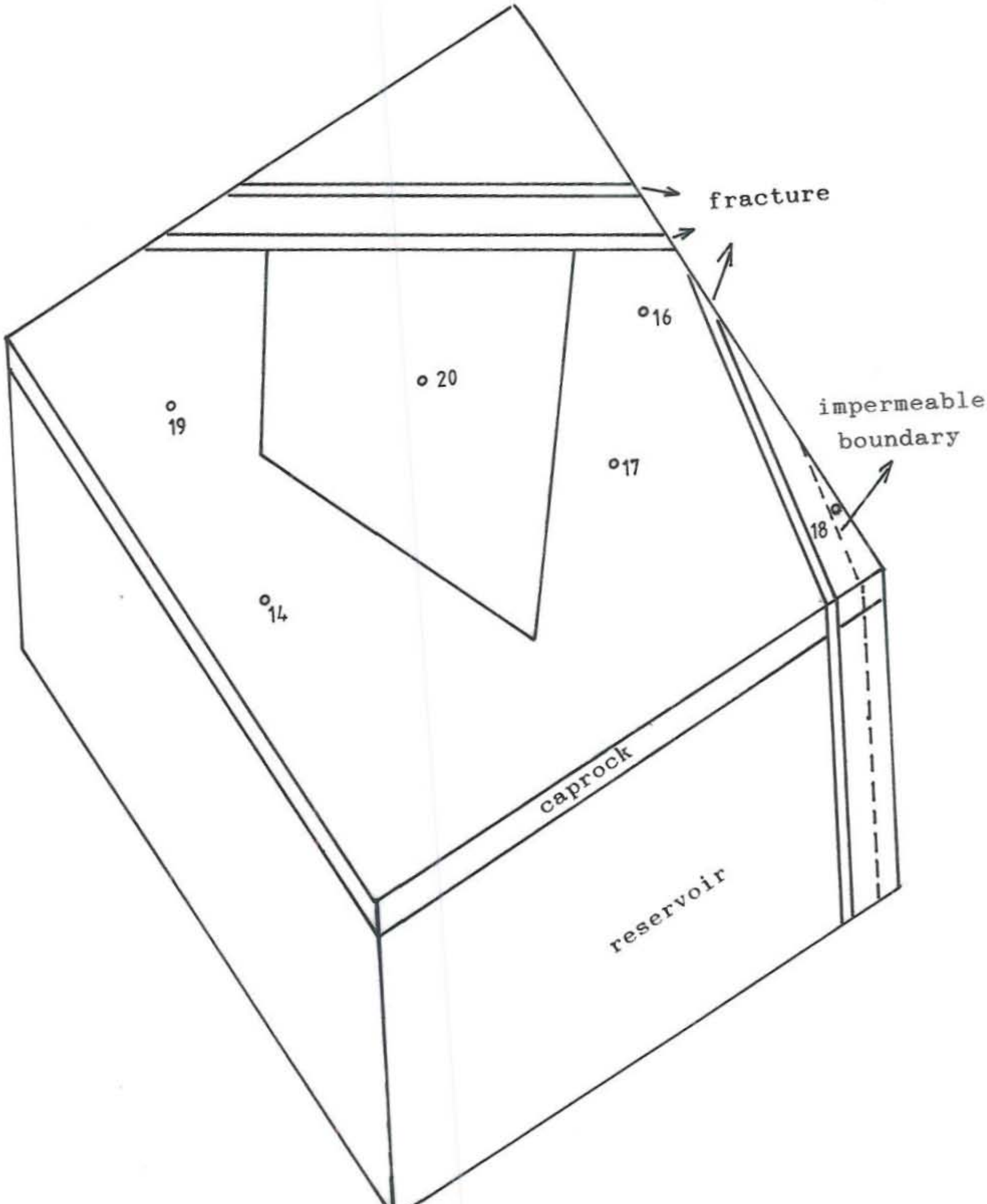


Figure 13 : Model used for simulation.

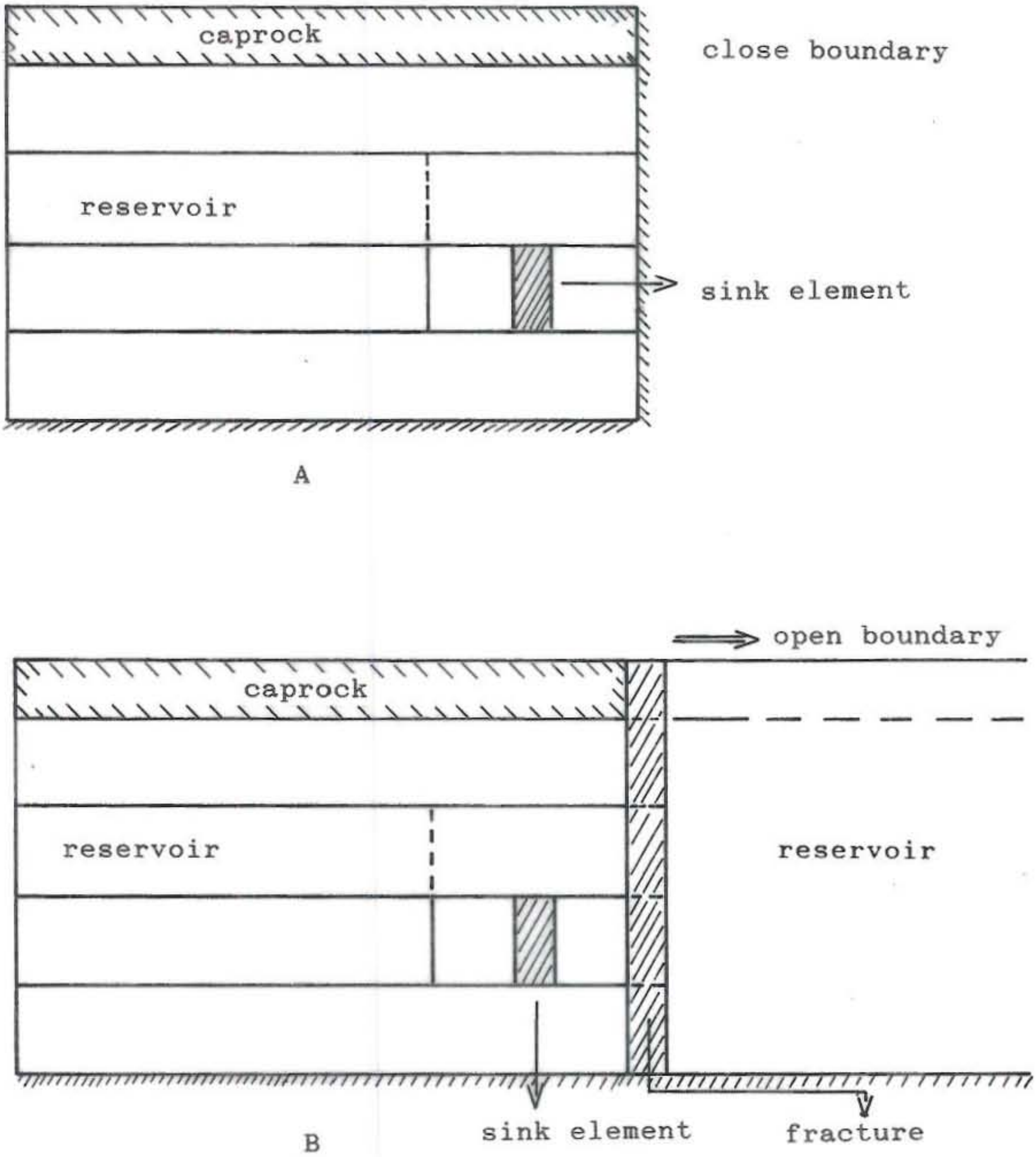


**Figure 14 : The South - North section of the simulation model. A. Closed boundary ; B. Open boundary toward North.**

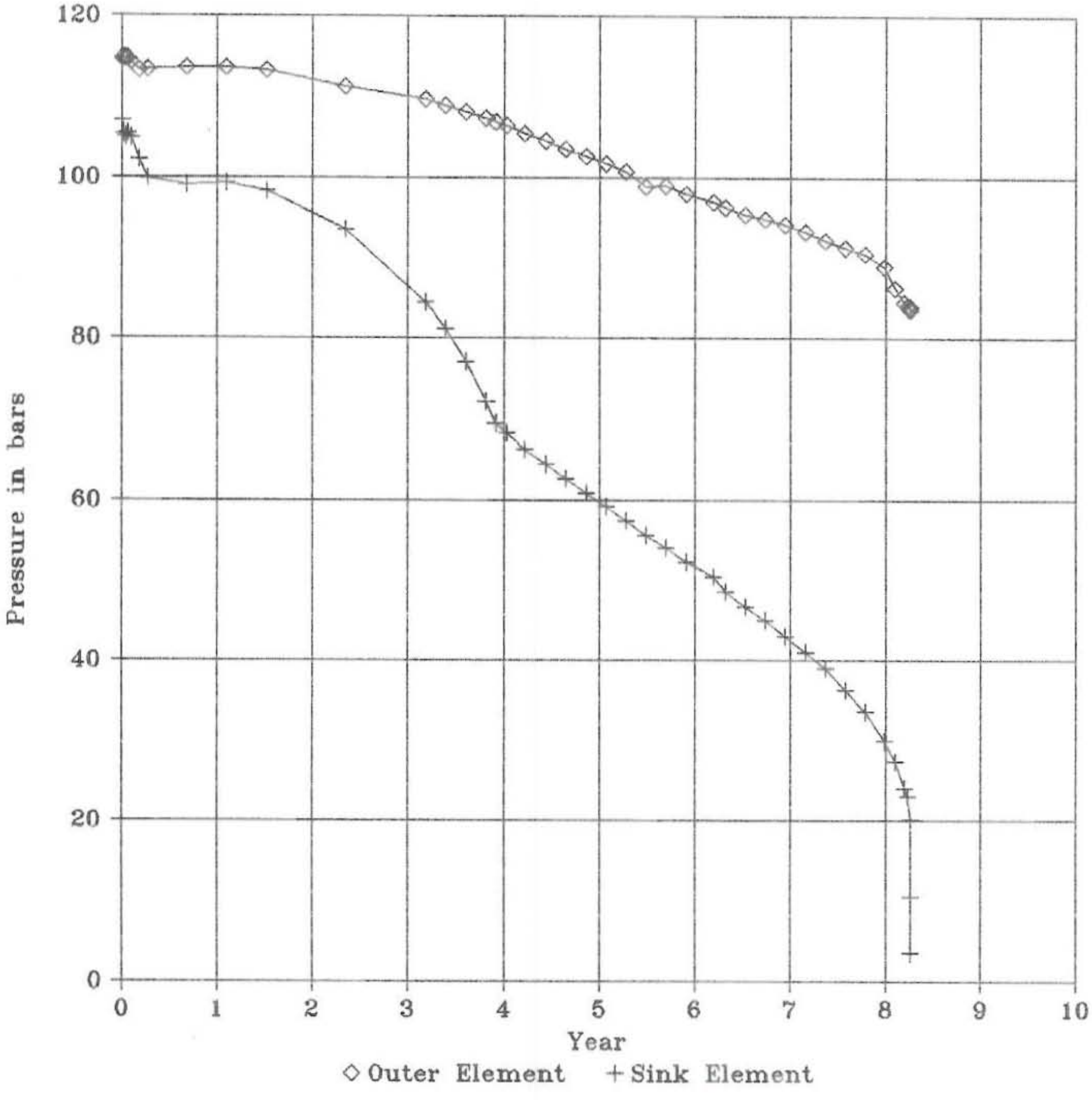


**Figure 15 : Pressure behaviour for the closed boundary case.**

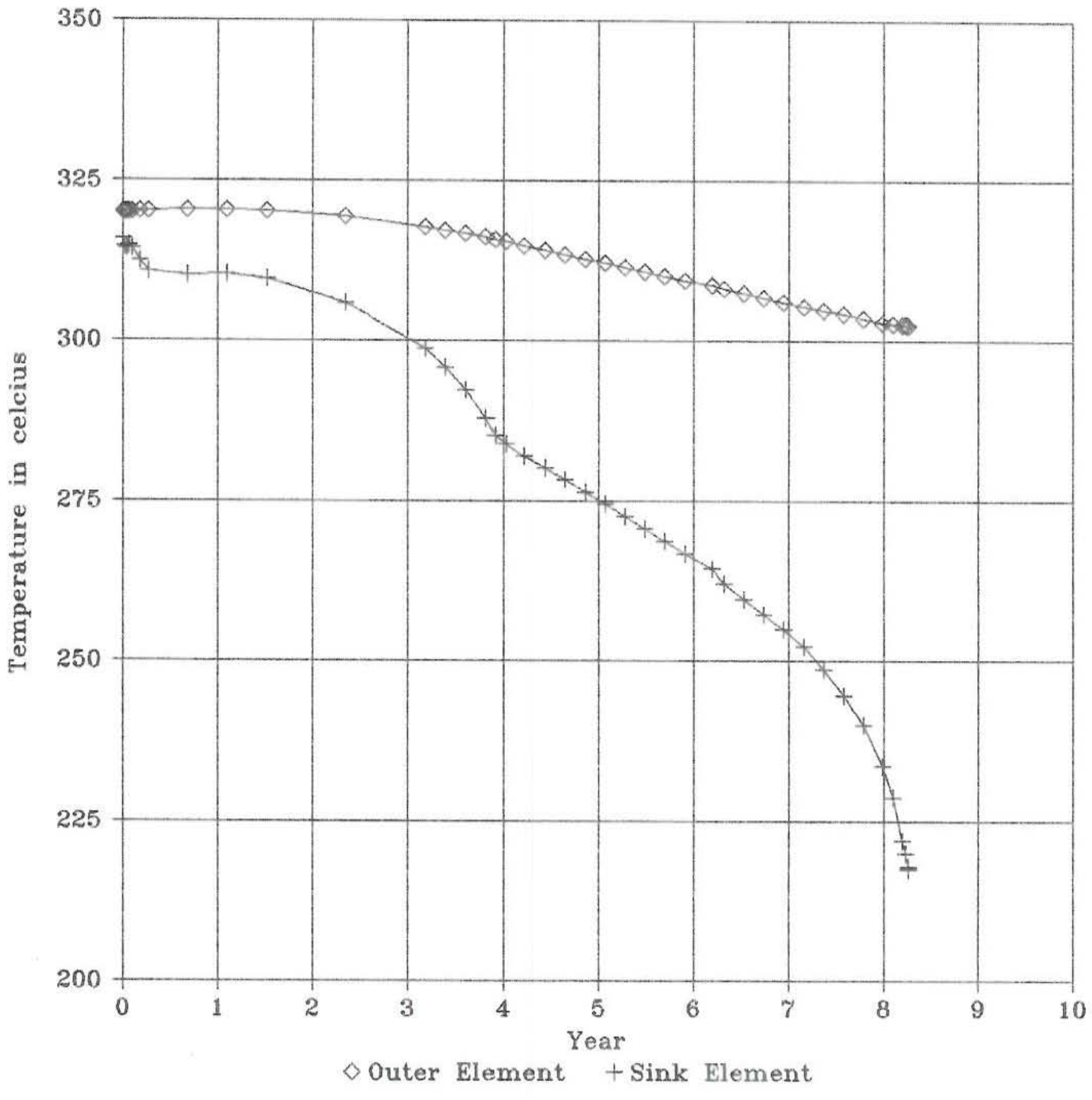


**Figure 16 : Temperature behaviour for the closed boundary case.**

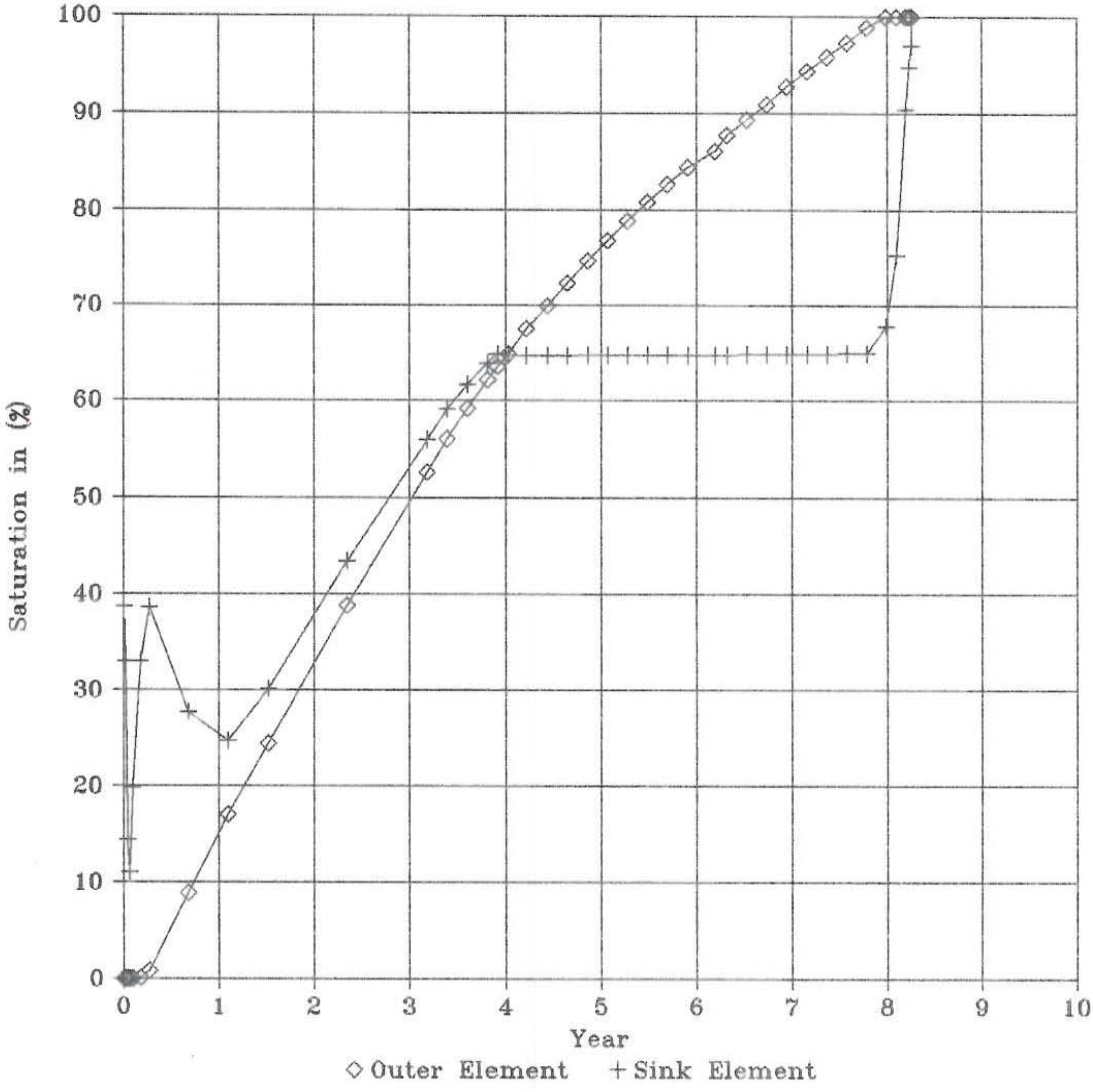


Figure 17 : Vapour saturation behaviour for the closed boundary case.

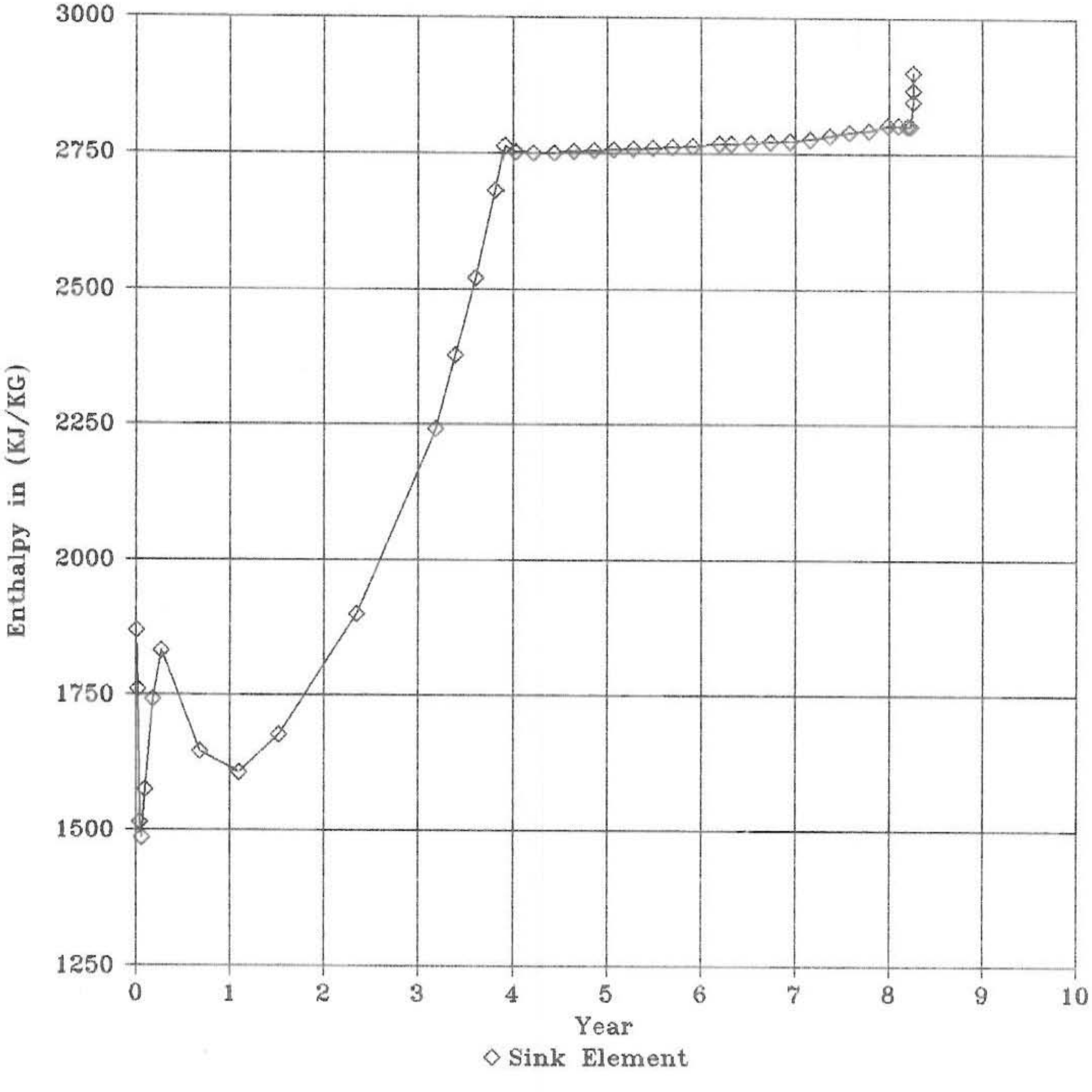


**Figure 18 : Enthalpy behaviour for the closed boundary case.**

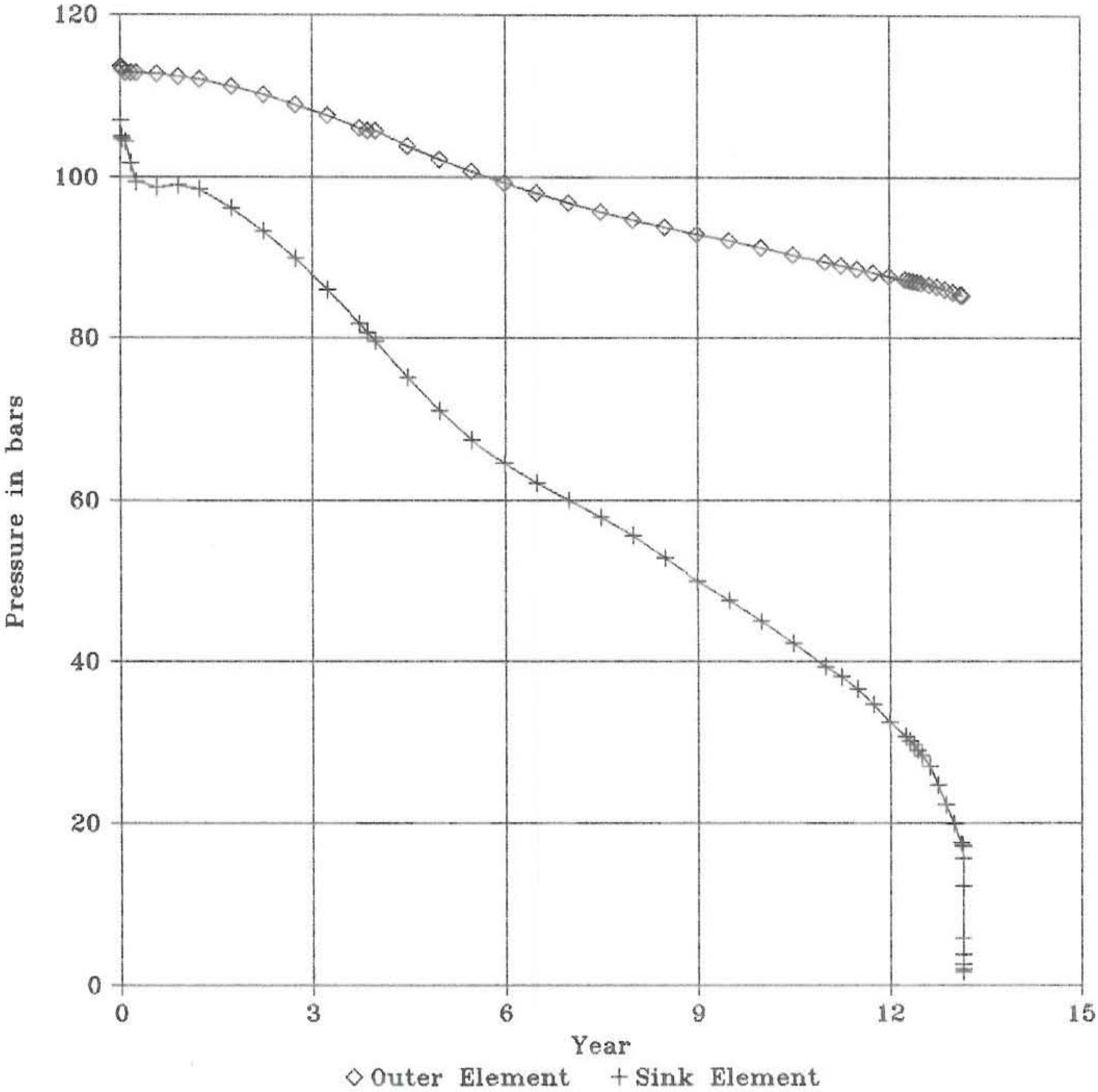


Figure 19 : Pressure behaviour for the open boundary case.

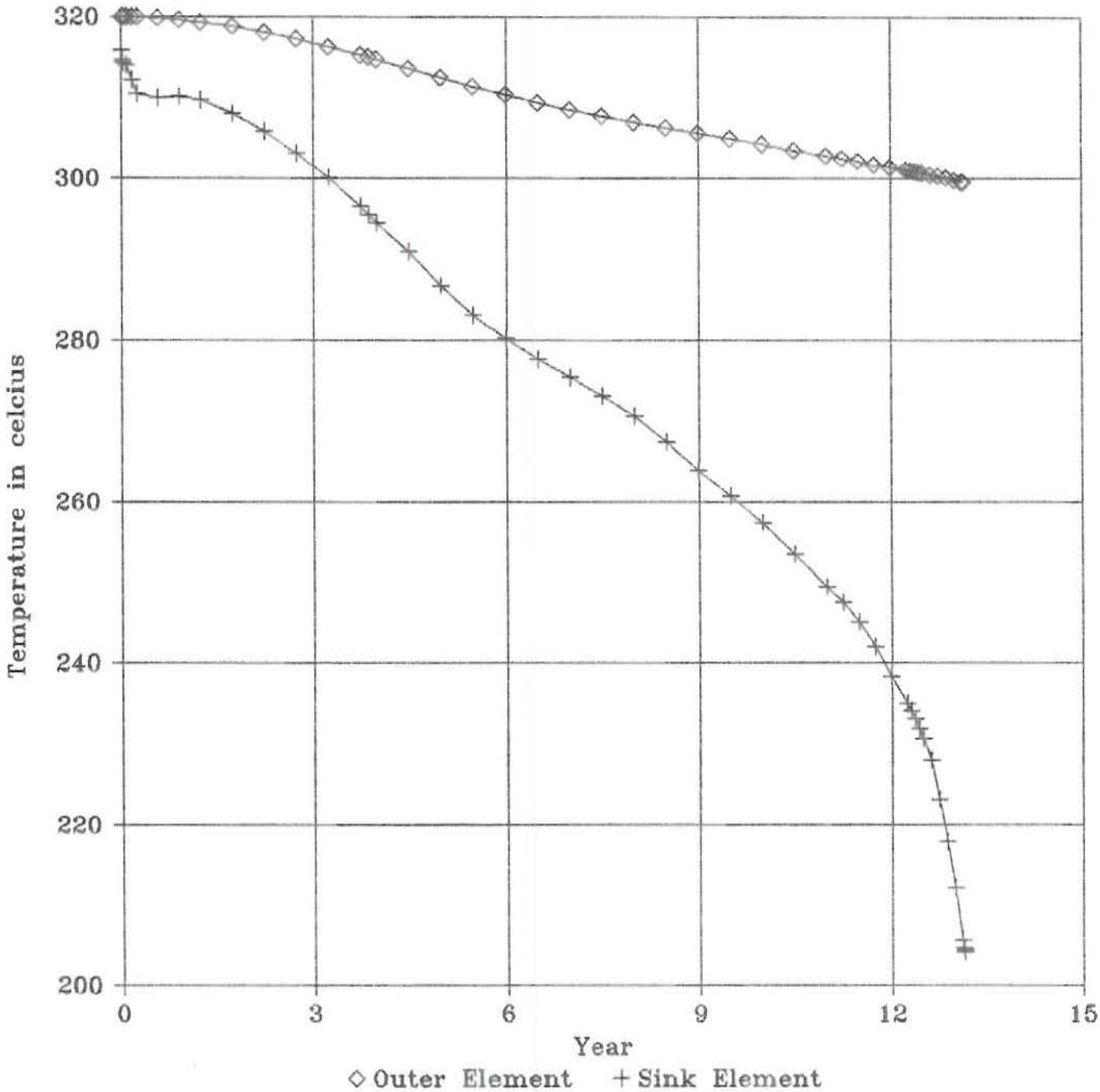


Figure 20 : Temperature behaviour for the open boundary case.

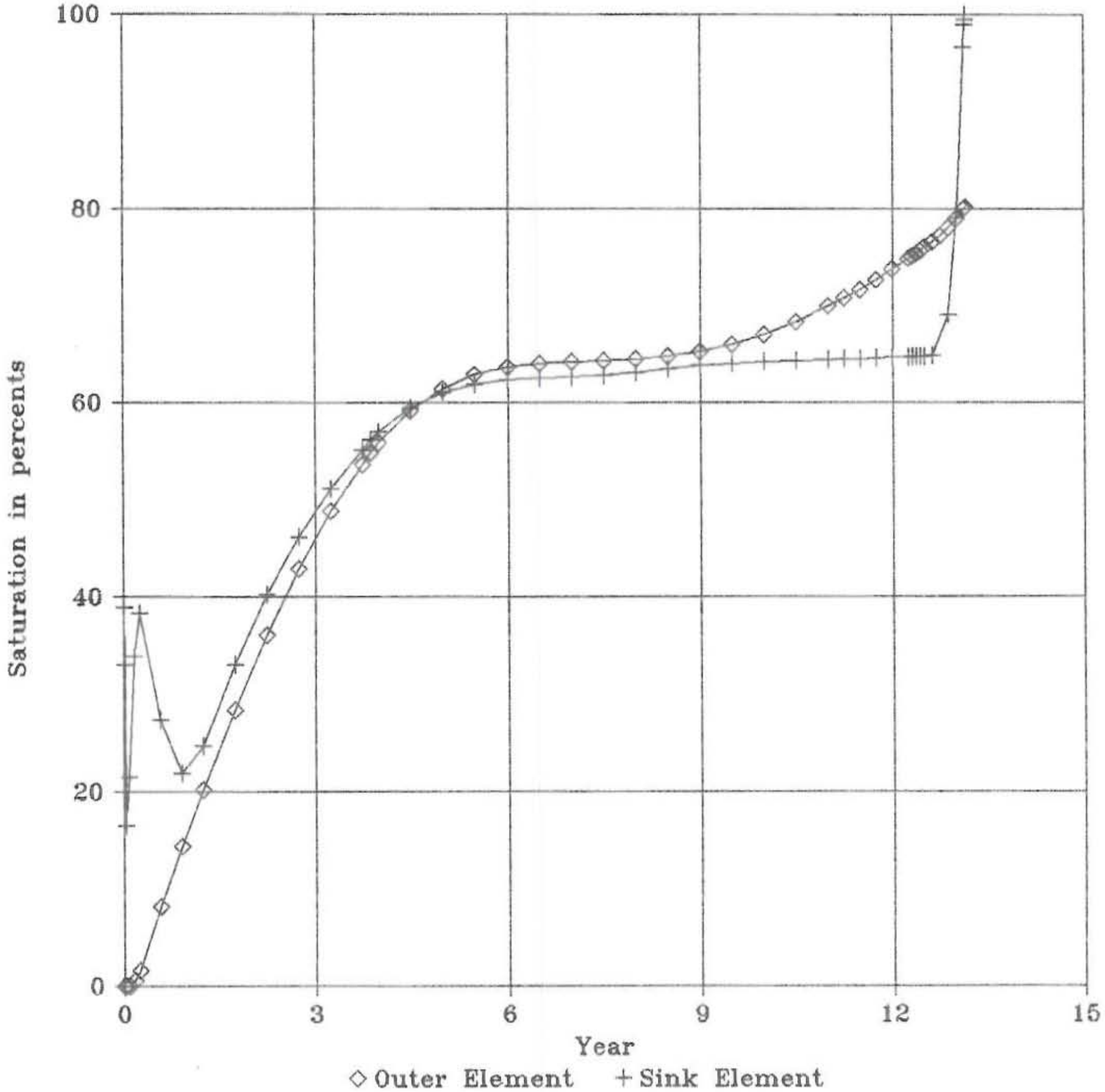


Figure 21 : Vapour saturation behaviour for the open boundary case.

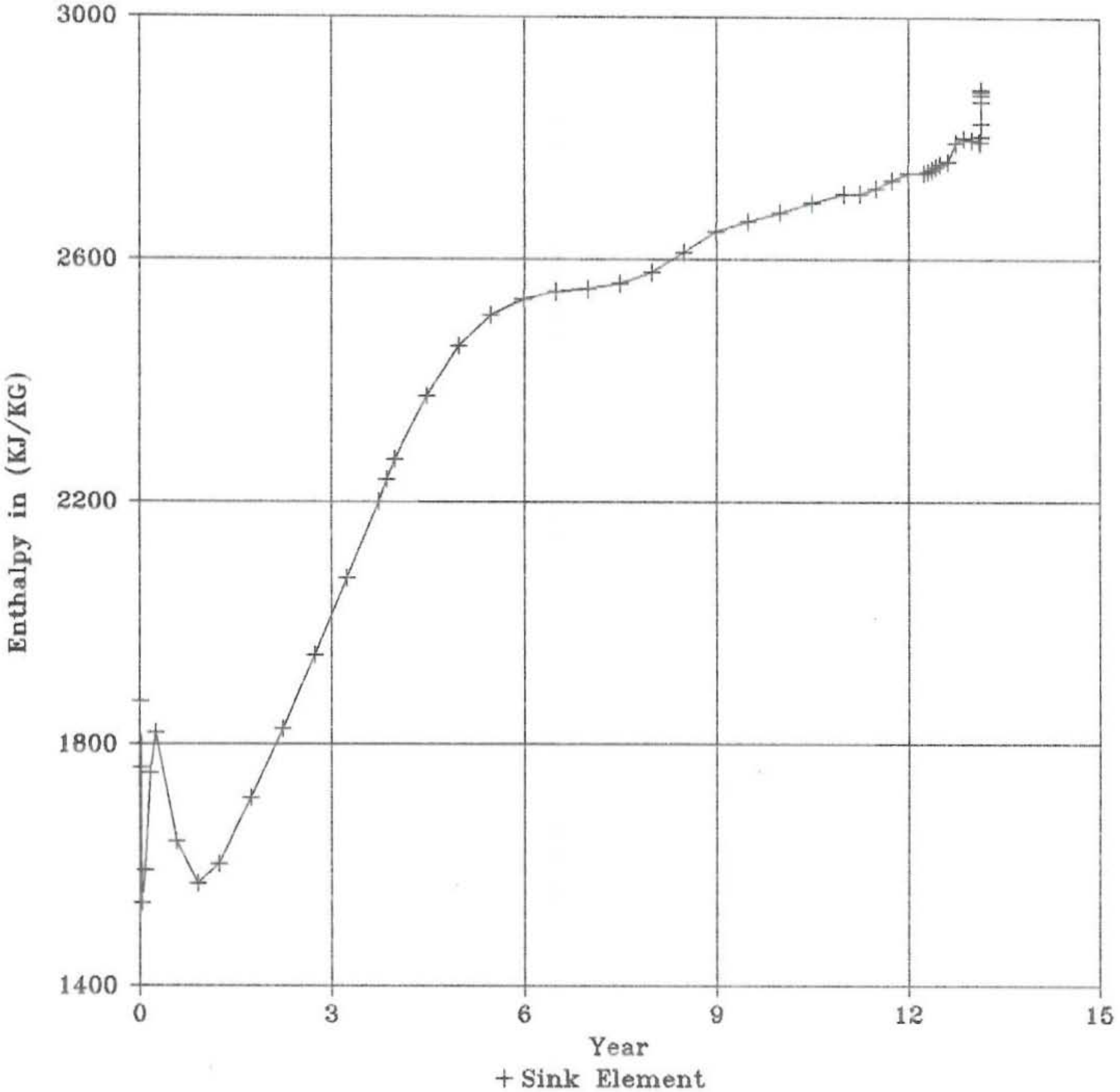


Figure 22 : Enthalpy behaviour for the open boundary case.